Science of the Total Environment 906 (2024) 167371

Contents lists available at ScienceDirect

Science of the Total Environment

journal homepage: www.elsevier.com/locate/scitotenv

Sources and controls of greenhouse gases and heavy metals in mine water: A continuing climate legacy

Alison M. Brown [a,b,*], Adrian M. Bass [b], Mark H. Garnett [c], Ute M. Skiba [a], John M. Macdonald [b], Amy E. Pickard [a]

[a] UK Centre for Ecology & Hydrology, Bush Estate, Penicuik, Midlothian EH26 0QB, UK
[b] School of Geographical & Earth Science, University of Glasgow, Glasgow G12 8QQ, UK
[c] NEIF Radiocarbon Laboratory, Rankine Ave, East Kilbride, Glasgow G75 0QF, UK

HIGHLIGHTS

- Water from abandoned coal mines contains high levels of carbon dioxide and methane.
- Mine water as a source of GHGs, needs recognition in greenhouse gas budgets.
- Methane sources were modern biogenic, thermogenic and coal-based hydrogenotrophic.
- Carbon dioxide sources were limestone, terrestrial organic carbon and coal.
- Mine water treatment removed Fe and As and partially removed Ni, Co and Mn only.

GRAPHICAL ABSTRACT

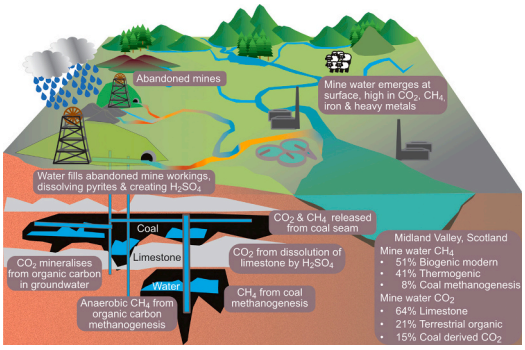

ARTICLE INFO

Editor: José Virgílio Cruz

Keywords:
Mine water
Methane
Carbon dioxide
Heavy metals
Greenhouse gas
Scotland

ABSTRACT

Water pollution arising from abandoned coal mines, is second only to sewage as a source of freshwater pollution and in coalfield catchments mine water can be the dominant pollutant, with oxidised iron smothering the bed of receiving rivers. This study measured greenhouse gases in mine water outflows from sixteen sites across the Midland Valley in Scotland. Radiogenic and stable carbon isotopes measurements ($\Delta^{14}C$ and $\delta^{13}C$) were used to determine the sources of both methane (CH_4) and carbon dioxide (CO_2) produced within the flooded mine environment. Concentrations of CH_4-C ranged from 20 to 215 μg l^{-1} and CO_2-C from 30 to 120 mg l^{-1}, with CO_2 accounting for 97 % of the mine water global warming potential. Methane origins included 51 % modern biogenic, 41 % thermogenic and 8 % from hydrogenotrophic methanogenesis of coal. The most significant inverse impact on biogenic CH_4 concentrations was sulphate, most likely due to sulphate reducing bacteria outcompeting methanogens. Carbon dioxide origins included 64 % from the dissolution of limestone, 21 % from terrestrial organic carbon and 15 % from coal. The limestone derived CO_2 was positively correlated with high sulphate concentrations, which resulted in sulphuric acid and caused the dissolution of carbonate from limestone. The mine waters experienced significant carbonate buffering becoming only slightly acidic (pH 6–7), but with significant loss of inorganic carbon. The mine waters had low dissolved oxygen (6–25 %) and high dissolved iron (2 to 65 mg l^{-1}) and manganese (0.5 to 5 mg l^{-1}) concentrations. Dissolved greenhouse gases from

* Corresponding author at: UK Centre for Ecology & Hydrology, Bush Estate, Penicuik, Midlothian EH26 0QB, UK.
E-mail address: albrown52@ceh.ac.uk (A.M. Brown).

https://doi.org/10.1016/j.scitotenv.2023.167371
Received 7 June 2023; Received in revised form 11 September 2023; Accepted 24 September 2023
Available online 25 September 2023
0048-9697/© 2023 The Authors. Published by Elsevier B.V. This is an open access article under the CC BY license (http://creativecommons.org/licenses/by/4.0/).

abandoned mines were estimated as 0.27 $^{+0.31}_{-0.18}$ % of Scotland's global warming potential. This novel work has contributed information about the sources and controls of greenhouse gas fluxes in mine waters and identified the need to quantify and report this emissions term.

1. Introduction

1.1. Acid mine drainage

In recent decades, heavy metal pollution has become a global environmental issue with implications for both environmental and human health, with mine water (MW) outflows from coal and metal mines constituting one of the major sources of heavy metal pollution to the aquatic environment (Fleming et al., 2021, 2022; Schwarzenbach et al., 2010; De Voogt, 2020; Wright et al., 2017; Younger, 2001). When in operation, water is pumped from the mine and the mine is ventilated. The introduction of oxygen oxidises pyrites (iron sulphide (FeS_2)) which accumulate on the mine walls. After mine closure, pumps are switched off, and water rises until it reaches the lowest discharge point (either the surface via old adits, springs and seepage or an overlying aquifer). This dissolves the accumulated salts, making the initial discharge from abandoned mines of very poor quality. Additionally when exposed coal seams are flooded, microorganisms can greatly accelerate the oxidation of mineral sulphides forming sulphuric acid, which subsequently dissolves any metal compounds present, resulting in high concentrations of Fe, Zn, Cu, Pb, Cd, Mn and Al (Dhir, 2018; Alhamed and Wohnlich, 2014; Stearns et al., 2005). Most of the pollution is from deep mines rather than opencast (Younger, 2001).

Mine water from abandoned mines, including coal mines, has been documented as globally, polluting water bodies including groundwater (Acharya and Kharel, 2020; Tomiyama and Igarashi, 2022). These impacts are likely to increase in future and be with us for many hundreds of years (Younger, 1997). China is the biggest producer of coal globally with its national production rising by over 10 % in 2020 to reach 4560 million tonnes, equivalent to 52 % of global production. Other countries that contribute >5 % of global coal mining production include the US, India, Australia, Russia and Indonesia (Energy Institute, 2023). While comprehensive figures for abandoned mines do not exist, South Africa has identified 6152, the United States >500,000, Australia >50,000 and the United Kingdom >2000, abandoned mines, covering all types of mine (Thisani et al., 2020). The number of abandoned coal mines in China is expected to reach 12,000 by 2020 (Lyu et al., 2022) with China the most seriously impacted country by mine water (Li, 2018).

In addition to being a source of heavy metals, MWs are supersaturated with greenhouse gases (GHG), including carbon dioxide (CO_2) and methane (CH_4). Where carbonate rock is present, the sulphuric acid generated in the mine dissolves the carbonate to produce CO_2. Elevated concentrations of CO_2 are common in discharges from abandoned coal mines (Hedin and Hedin, 2016; Vesper et al., 2016; Jarvis, 2006), though its contribution to global GHG budgets remains uncertain. As the carbonate dissolves, the acid is neutralised, the pH typically rises to around pH 6 (reducing the environmental impact) and MW becomes supersaturated with CO_2 (of a fossil origin) with high inorganic carbon loading in the form of bicarbonate. Where limestone is not present in the mine, it is often added to the treatment process to aid neutralisation (Dhir, 2018; Watten et al., 2005) also producing CO_2. Additionally CO_2 may be produced by in-water mineralisation of modern dissolved organic carbon (DOC) in groundwater (Winterdahl et al., 2016), and CO_2 may be associated directly with ancient coal seams which could transfer into the MW (Iram et al., 2017).

Details of CH_4 released in MW are currently poorly constrained. The production mechanisms are not necessarily simple but there are likely two main mechanisms encompassing three sources: thermogenic CH_4 from the coal seams (degradation of coal due to high temperature and pressure) and biogenic CH_4 from both ancient and modern carbon sources, which may progress via acetoclastic (using acetate) or hydrogenotrophic (using CO_2 and hydrogen (H_2)) methanogenesis (Gonzalez Moguel et al., 2021; Mayumi et al., 2016; Meslé et al., 2013). Thermogenic CH_4 is associated with all coal seams, with deeper and older coal seams typically containing more CH_4 than shallower younger seams (IEA, 2020). Once underground mines flood, the hydrostatic pressure on the coal seams stabilises and CH_4 emissions are estimated to continue until the mines are completely flooded (Fernando, 2011). However, CH_4 emissions can continue where workings remain above the recovered water levels and pockets of CH_4 can be trapped by rising waters (Kershaw, 2005). Projections of global coal mine CH_4 emissions to 2100, estimate a 4-fold increase from active underground mines and an 8-fold increase from abandoned mines (Kholod et al., 2020a), though this does not account for CH_4 dissolved in the MW which subsequently evades to the surface. The rate of CH_4 emissions from abandoned coal mines was linked to the size of the remaining CH_4 reserve, with CH_4 content increasing with depth (Kershaw, 2005). Hence emissions of CH_4 in MW could be associated with dissolution of thermogenic CH_4 despite its low solubility. Biogenic CH_4 production may occur because of the presence of methanogenic bacteria in the MW, with anaerobic biodegradation of either coal substrate or modern organic material accumulating in the mines or from groundwater (Gonzalez Moguel et al., 2021). Microbial degradation of coal to produce CH_4 (coal methanogenesis) is another potential source but the irregular structure of coal and the complex microbial consortia, requiring specific conditions, make it unlikely to occur at all locations. This mechanism has been more commonly found in more volatile grade coals (lignite and bituminous) compared to anthracite found in Scotland (Iram et al., 2017), and would necessarily occur before dissolution of Fe^{2+}, a strong electron donor, inhibited methanogenesis (Furukawa et al., 2004). All three mechanisms for CH_4 production are plausible and could occur synchronously.

The different CO_2 and CH_4 pathways leading to subsurface GHG generation will result in different isotopic signatures. For example, CO_2 and CH_4 from ancient sources will no longer contain ^{14}C and the mechanism of production will impact the amount of ^{13}C depletion (Lopez et al., 2017). In this context, carbon radiogenic and stable isotope concentrations ($\Delta^{14}C$ and $\delta^{13}C$) are powerful tools for understanding CO_2 and CH_4 sources, which could inform measures to reduce emissions to atmosphere either within the mine or treatment process with clear implications for climate.

1.2. Mine water treatment approaches

The generation of low pH MW enhances the dissolution of heavy metals (Saria et al., 2006; Florence et al., 2016), with concentrations likely impacted by geology, flow conditions and MW temperatures. However, water from abandoned mines often contains a predominance of calcium bicarbonate ($Ca(HCO_3)_2$ and calcium sulphate ($CaSO_4$). The dissolution of these minerals increases pH, consumes hydrogen ions and releases calcium (Ca^{2+}), magnesium (Mg^{2+}) and bicarbonate (HCO_3^-). The main environmental hazard of MWs is therefore not low pH but the high concentration of dissolved Fe(II) associated with low oxygen conditions. When the MW reaches the surface the soluble Fe(II) reacts with oxygen to produce insoluble Fe(III) and this process significantly depletes dissolved oxygen from rivers and streams, producing an orange iron precipitate (Johnston et al., 2008). Most treatment systems are designed to achieve the oxidation and subsequent precipitation as Fe(III) prior to discharge to the environment.

Wetlands are often used to treat MW as they can absorb and bind heavy metals depending on soil, substrate, hydrology and vegetation. This involves: settling, sedimentation, adsorption, oxidation and hydrolysis of metals and precipitation of metal carbonates and sulphates or anaerobic conversion to metal sulphides and biological removal of heavy metal in the wetlands by plant uptake (Sheoran and Sheoran, 2006). There are variations on the standard treatment approach, dependent on space available, site geography and topography and the requirement to minimise energy usage (The Coal Authority, 2017). The process is primarily designed for the removal of Fe and not specifically for removal of heavy metals or GHGs. Different stages may both promote or reduce GHG release to the atmosphere. There are typically three stages in the treatment process with the different treatment options shown schematically in Fig. 1.

1. Oxygenation of the water either via a gravity cascade or chemical oxidation, for example, adding peroxide, primarily to change dissolved soluble Fe^{2+} (ferrous) to insoluble Fe^{3+} (ferric).
2. Passing the water to a deep lagoon where the insoluble Fe^{3+} has time to settle out.
3. Passing the water through a series of reed beds to filter out fine Fe^{3+} particles.

While research on methods to minimise the impact of acid mine drainage have been ongoing for over 50 years (Verburg et al., 2009), MWs from many abandoned mines globally are not treated. This can be dependent on land-use history, climate, topography, hydrogeology, available technology, socio-political outlooks, environmental scientists and regulatory agencies (Acharya and Kharel, 2020). Global data pertaining to treatment are not available but some data is available at national scale. For example significant MW pollution is reported for the USA, a legacy of how the mining industry has operated, with average flows of 190,000 m^3d^{-1} of contaminated MW, with around 76,000 m^3d^{-1} untreated, entering the environment from 43 mining sites under federal oversight (Brown, 2019).

GHG emissions from MW could be influenced by the treatment approach. For example the use of chemical oxidation may provide an opportunity for oxygenation of CH_4 by methanotrophs and the absorption of the CO_2 by reeds, whereas direct outgassing occurs in a gravity cascade. Sediments within the deep anoxic lagoons could support methanogens, whereas methanotrophs could be supported in the water column, with various forms known to be associated with natural gas (Topp and Pattey, 1997). Burial of inorganic and organic carbon may occur within the mud, but how the mud is disposed of will determine potential carbon capture. MW treatment shallow-water reed beds are a

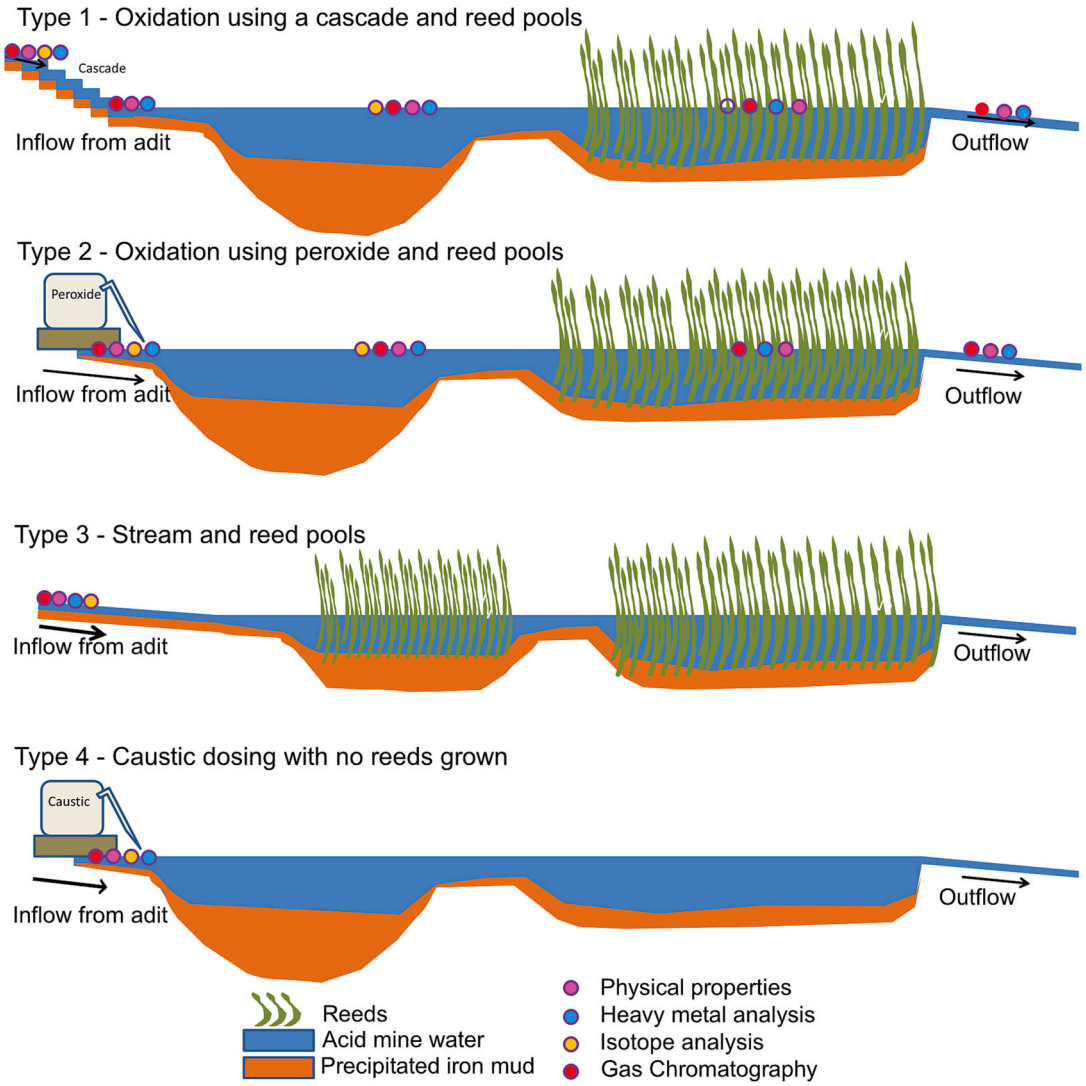

Fig. 1. Schematic of main mine water treatment process options used across the measurement sites. The pink, blue, yellow and red indicate where different types of measurements were made. Details of which locations used which treatment approach are included in Table 1. In type 4 caustic (sodium hydroxide) dosing is used both to oxidise and neutralise the mine waters.

wetland environment and may absorb CO_2 and release CH_4 (Laanbroek, 2010) as wetlands are the highest natural source of CH_4 (Gauci et al., 2010; Peng et al., 2022). Conversely reed-bed may act as a conduit for soil-produced CH_4 passing to the atmosphere or support methanotrophs reducing CH_4 evasion (Macdonald et al., 1998). This complex interplay of processes requires further investigation to determine the potential significance of GHGs in MW.

Given the global challenge presented by pollution from MW, but inadequate understanding and quantification of MW GHG dynamics, further insight into their sources and mechanisms could support remediation approaches with multiple benefits including GHG management. This study addressed the following key questions: (1) can the origins of the MW CH_4 and CO_2 be determined from stable and radiogenic isotopes measurement, (2) what controls variation in MW CH_4 and CO_2 composition and concentration and (3) do different treatment processes, specifically the use of peroxide or cascade, and varied use of pools and reed beds, minimise GHGs release to the atmosphere improve heavy metals removal.

To investigate these questions the Midland Valley in Scotland, a historical coal mining region, was selected for this study. Water pollution arising from abandoned coal mines is second only to sewage as a source of freshwater pollution in Scotland and in many coalfield catchments it is the dominant pollutant source (Younger, 2001). Nine percent of rivers in England and Wales, and 2 % in Scotland fail to meet their Water Framework Directive targets of good chemical and ecological status due to abandoned mines and carry high levels of Cd, Fe, Cu and Zn (Johnston et al., 2008). The Coal Authority manages over 75 MW treatment schemes across Britain, treating over 122 billion litres of MW every year (The Coal Authority, 2017), although not all MW is treated at present.

2. Materials and method

2.1. Geology and study area

Coal bearing rocks in Scotland date from the Carboniferous and trend from southwest (covering the Ayrshire coast to Glasgow) to the northeast (covering the Edinburgh area and the Fife coast) and identified as the Midland Valley of Scotland. These rocks are bounded by the Highland Boundary Fault to the northwest and the Southern Upland Fault to the southeast (Leslie et al., 2016). Most stages of the Carboniferous are present, with the coal-bearing Namurian strata from the Clackmannan Group. Limestone is both above, below and within the coal measures (Leslie et al., 2016; Dean et al., 2011).

Sixteen identified MW outflows were selected from across the Midland Valley, some of which had treatment systems and others which discharged directly into rivers or streams (Fig. 2), with full details of the survey locations included in Table 1 and additional site information included in the supplementary information Fig. A.1. All of these sites are considered to be in the Limestone Coal Group or the Lower Limestone Coal Group with the exception of MA2 which is considered to be in Productive Coal Measures and MA4 which covers all coal measures from outcrop in the west to the deepest undersea workings in the east (Whitworth et al., 2012). The mines within this survey were closed between 1800 and 1989 (the last being MA6 closing in 1989 and MA4 which closed in 1988 but continued to be pumped until 1995). Many mines closed in the period 1955 to 1974. All the mine locations have been recovering over the last 30–220 years, and assumed to be fully flooded, although at some locations pumping is deployed to prevent the MW from contaminating groundwater.

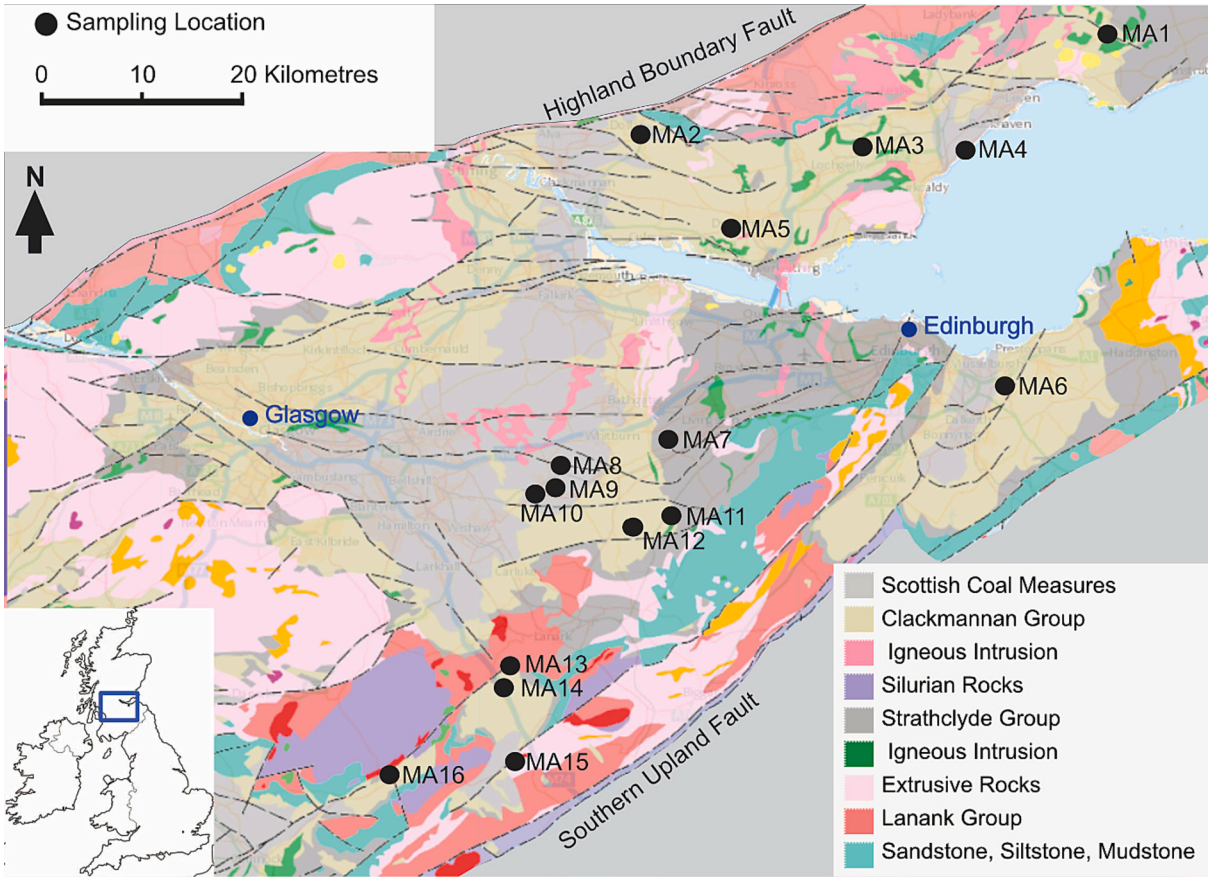

Fig. 2. Sample site locations (MA1 to MA16) shown in the relation to the geology of the Midland Valley, Scotland.
(Faults and bedrock geology were derived at a scale of 1:625,000 from https://mapapps2.bgs.ac.uk/geoindex/home.html (British Geological Survey, 2023).)

Table 1
Mine water sampling location, treatment, geology and hydrology.

No	Location code[1]	Latitude (N)	Longitude (W)	Height (m asl)	Mine or mine water locations name	Treatment[2]	Last known mining date[4]	Source Coal[3],[4]	Flow (l/s) [4]	Iron (mg l−1)[4]	pH[4]
1	MA1	56°14′45.06″	2°51′56.68″	145	Lathallan Mill	Treated (3)	Unknown	LCG	12	12.8	N/A
2	MA2	56° 9′30.24″	3°38′36.52″	35	Mains of Blairingone	Treated (3)	1900s–1954	PCM	5–15	10–25	N/A
3	MA3	56° 8′20.60″	3°16′51.52″	75	Minto	Treated (3)	1967	LCG	40–80	12	N/A
4	MA4	56° 8′1.15″	3° 6′45.45″	50	Frances	Treated (4)	1988, (Pumping stopped 1995)	Multiple	120	40–120	6.2
5	MA5	56° 3′36.90″	3°30′6.14″	40	Pitfirrane	Treated (3)	1800, recent opencast	LCG	200–400	3	N/A
6	MA6	55°53′38.10″	3° 3′40.39″	35	Bilston (Junkies Adit)	Discharged	Lady Victoria 1981, Easthouses 1969, Lingerwood 1967 Connected to Bilston 1989	LCG	46	7	N/A
7	MA7	55°50′53.67″	3°36′49.78″	175	Cuthill	Treated (1)	1962	LLCG	5–15	10–30	N/A
8	MA8	55°49′3.96″	3°47′40.92″	200	Shotts	Discharged	1968–1974	LCG	240	1.6	7.1
9	MA9	55°47′59.39″	3°48′50.64″	200	East Allerton	Treated (3)	Unknown, recent opencast	N/A	N/A	N/A	N/A
10	MA10	55°47′43.31″	3°49′40.28″	200	Kingshill	Treated (1)	1974 and 1968	LCG	11.6	11.6	7
11	MA11	55°46′15.03″	3°37′0.78″	240	Pool Farm	Treated (2)	1955	LCG	30–100	10–20	N/A
12	MA12	55°45′40.04″	3°40′36.95″	260	Mousewater	Treated (2)	1955	LCG	30–70	10–30	N/A
13	MA13	55°36′57.91″	3°52′49.97″	210	Johnhill burn [5]	Discharged	Recent opencast - Broken Cross Auchlochan No. 9, 1968,	LCG	N/A	N/A	N/A
14	MA14	55°35′58.21″	3°53′24.73″	225	Muirburn [6]	Discharged	Auchlochan 1968, Coalburn 1962, recent opencast	LCG	N/A	N/A	N/A
15	MA15	55°31′26.18″	3°52′32.54″	225	Glentaggart	Discharged	Glentaggart 1969, recent opencast	N/A	22	4.18	7.12
16	MA16	55°30′43.73″	4° 5′3.35″	215	Kames	Treated (1)	1968	LCG	15–20	15	6.8

Notes
1. Locations code: MA- indicates this survey (Mine Adits) and the location code the number from 1 to 16 represents the position on this survey, with 1 furthest north and the 16 furthest south.
2. The number in brackets in the treatment column refers to the treatment arrangement as described in Fig. 1; (1) cascade, (2) peroxide (3) stream and no deep-water pool and (4) caustic with no reeds.
3. LCG = Limestone Coal Group, LLCG = Lower Limestone Coal Group, PCM = Productive Coal Measures
4. Indicative coal measure, flow, pH and iron concentration is from - The Coal Authority Overview of Mine Water in the UK Coalfields- Advice on Mine Water recovery and Mine Gas (November 2012) (Whitworth et al., 2012), however these values can change with time.
5. Johnhill was measured in the receiving stream (Johnhill burn) as mine water pollution was via seepage with the source unidentified.
6. Muirburn was measured in the receiving stream as the source was not accessible as it is surrounded by wetland and the mine water is likely diluted at the measurements point.

2.2. Data collection and analysis

Between July and September 2022, sixteen MW outflow sites (MA1–MA16) were sampled for dissolved GHG concentrations, water physiochemical properties, carbon stable and radiogenic isotopes of the CO_2 and CH_4 and metal concentrations (Brown et al., 2023). At most locations measurements could not be made directly in the outflow and samples were collected via a bucket at the nearest possible access location to the source. Additionally, four treatment locations, two using a cascade (MA7 and MA10) and two using peroxide (MA11 and MA12), were sampled throughout the treatment reed pools to determine the impact of treatment processes on both GHG processing and heavy metal removal. Carbon stable and radiogenic isotopes of the CO_2 and CH_4 were sampled in these reed pool systems for comparison with each source, to determine if retention of CH_4 and CO_2 within the reed pools impacted exchange of carbon between CH_4 and CO_2 or whether additional CH_4 and CO_2 were generated. Use of peroxide instead of a cascade slows the GHG outgassing to atmosphere. To further understand oxygenation and outgassing in the cascade systems, one system MA7, which had the most efficient oxygenation cascade, was sampled throughout the cascade. This cascade had 71 steps, each with a length of 0.76 m and a drop of 0.16 m with the water taking 65 s to traverse the cascade. A study of this system, with water sampled every 11 steps enabled the effect of oxygenation and outgassing to be determined on GHGs concentrations. Sample collection in the cascade caused some additional turbulence, but it was assumed to be the same for each measurement point.

Dissolved gas samples were collected in triplicate at each location using the headspace method, together with ambient air samples (Billett and Moore, 2008). Conductivity (Cdt), temperature (T_W), dissolved oxygen concentration (DO), dissolved oxygen saturation (DO%) and pH were measured 0.1 m below the water surface using a HQ40d Multi portable meter (Hach) with a Intellical CDC401 Laboratory 4-Poles Graphite Conductivity Cell, a Intellical LDO101 Laboratory Luminescent/Optical Dissolved Oxygen and a PHC10101 Combined pH electrode. A two-litre water sample was retained for later analysis which was kept in a cool-box until returned to the laboratory for processing. Sample filtration and processing was undertaken on the same day as collection.

Headspace samples were analysed using an Agilent 7890B gas chromatograph (GC) and 7697A headspace auto-sampler (Agilent, Santa Clara, California), with CO_2, CH_4 and nitrous oxide (N_2O) concentrations determined by running gas vials containing four mixed gas standards prepared in a consistent way to the ambient air samples. The concentrations of the standards gases were: 1.12 to 98.2 ppm for CH_4; 202 to 5253 ppm for CO_2; and 0.208 to 1.04 ppm for N_2O. Water samples were filtered within 8-h of collection through a Whatman GF/F 0.7 μm, under vacuum. Filtrate was then analysed for: total dissolved nitrogen (TDN), total dissolved carbon (TDC) and dissolved organic carbon (DOC) and anion & cation concentration. Analysis for TDN, TDC and DOC were undertaken using a Shimadzu TOC-L series Total Organic Carbon Analyser with all samples run within 24-h of collection. The

difference between TDC and DOC was used to calculate dissolved inorganic carbon (DIC). The filtration prior to measurement resulted in outgassing of any CO_2 raising the pH, such that most DIC measured by this method was in the form of HCO_3^- and will underestimate the total DIC in the original sample. TOC measurement accuracy was impacted by high DIC concentrations (Findlay et al., 2010), which was corrected for, but has increased the TOC uncertainty. Ion chromatography using a Metrohm 930 Compact IC Flex was undertaken to determine both anion and cation concentrations. A mixed ion standard containing 11,000 ppm chloride (Cl^-), 5000 ppm nitrate (NO_3^-), 4000 ppm sulphate (SO_4^-), 10,000 ppm sodium (Na^+), 5000 ppm ammonium (NH_4^+), 1000 ppm potassium (K^+), 1000 ppm calcium (Ca^{2+}) and 1000 ppm magnesium (Mg^{2+}), was diluted to make 8 standard solutions for calibration. These included dilutions of 0.1, 0.5, 1, 2, 5, 10, 25 and 50 %. ICP-MS was conducted by Edinburgh University on both filtered and unfiltered samples to determine concentrations of a large range of heavy metals. Agilent 7900 ICP-MS was used to produce a semi-quant scan of each sample in addition to the full quant data for all elements of interest including: Li, Be, B, Na, Mg, Al, Si, P, K, Ca, Ti, V, Cr, Mn, Fe, Co, Ni, Cu, Zn, Ga, As, Se, Rb, Sr, Nb, Mo, Ag, Cd, Sb, Cs, Ta, Hg, Pb and U. Concentrations presented are derived from for isotopes with the highest relative abundance. Multi-element calibrations were run at 6 dilutions at the start and every 15 samples.

2.3. Gas partial pressures

To calculate dissolved gas concentrations and partial pressures from the headspace equilibration method the following mass-balance equation was applied (Hamilton, 2006).

$$(C_{0liq})\cdot(V_{liq}) + (C_{0gas})\cdot(V_{gas}) = (C_{liq})\cdot(V_{liq}) + (C_{gas})\cdot(V_{gas}) \quad (1)$$

where: C_{0liq} and C_{0gas} are the original gas concentration, C_{liq} and C_{gas} are the concentrations in the liquid and gas phases after equilibration (shaking) and V_{liq} and V_{gas} are the volumes of the liquid and gas in the syringe (assumed to be the same before and after shaking). Assuming equilibrium inside the vessel then C_{liq} can be replace by:

$$C_{liq} = P_{gas}\cdot\beta_T\cdot P_{BAR} \quad (2)$$

where: P_{BAR} is the barometric pressure at the measurement time and altitude, Pgas is the partial pressure in the gas phase, β_T is the Bunsen solubility coefficient as a function of temperature. This can be rearranged:

$$(C_{0liq}) = (P_{gas}\cdot\beta_T\cdot P_{BAR}) + (C_{gas} - C_{0gas})\cdot(V_{gas})/(V_{liq}) \quad (3)$$

This gas concentration in μmoles L^{-1} can be converted to units of ppmv using the Ideal Gas Law, where ppmv = (μmoles L^{-1}). (RT), where R is the gas constant and T temperature in Kelvin.

This method can lead to errors in CO_2 estimates as dissolved CO_2 is in dynamic chemical equilibrium with other carbonate species. However, for these over-saturated MW samples with pH typically <6.5, the error was estimated to be <5 % and no corrections were applied (Koschorreck et al., 2021). One concern in the study design was that MW GHGs could outgas prior to measurement. This occurred due to the level of supersaturation resulting in observed bubble formation (MA4), turbulence induced by sample collection (MA7 and MA11) and transfer by pipe to the measurement location (MA2 and MA5). The results presented here therefore represent minimum GHG concentrations. Where rapid outgassing of CO_2 does occur the effect of carbonate buffering resulted in an increase in pH and some of the DIC converting to CO_2. The known relationships of carbonate chemistry in water can be used to determine if CO_2 outgassing is occurring before source measurement, allowing the theoretical CO_2 concentration to be determine from the measured pH and DIC concentration (Millero et al., 2006).

2.4. Radiogenic and stable carbon isotopes

Collection of samples for the radiogenic and stable carbon isotopes analysis of CO_2 and CH_4 required processing of sufficient water to collect a minimum of 2 mg of carbon for each gas. Evacuated accordion containers were used to collect water for isotopic analysis. A slow pump was used to gently fill the container (to minimise degassing), with between 5 and 6 l of water. One litre of CO_2-free air was added to the water container, which was shaken for 2 min to equilibrate the headspace. The headspace was subsequently collected in gas tight bags for analysis (Garnett et al., 2016). Stable ($\delta^{13}C$) and radiogenic ($\Delta^{14}C$) carbon isotopes were measured at the National Environmental Isotope Facility at East Kilbride. To distinguish between the possible sources of CH_4 and CO_2, both radiogenic ($\Delta^{14}C$) and stable ($\delta^{13}C$) isotope measurements were required and analysis was undertaken by assuming a three-source model (Fig. 3) (Gonzalez Moguel et al., 2021; Keith and Weber, 1964; Iram et al., 2017; Lu et al., 2021).

To determine the proportions of the different CH_4 and CO_2 sources the following assumptions were made: (1) any CH_4 from thermogenic or ancient carbon methanogenesis and any CO_2 from limestone or coal would have no measurable ^{14}C, (2) any CH_4 from modern biogenic methanogenesis and any CO_2 from terrestrial DOC mineralisation would be of modern origin and exhibit no significant loss of ^{14}C, (3) the $\delta^{13}C$ signals from all CH_4 and CO_2 sources were the same across the Midland Valley region and (4) there was no isotopic fractionation of the CO_2 when produced from limestone. However, once in the aqueous phase, the CO_2 will fractionate from the HCO_3^- with more ^{13}C in the HCO_3^- than the CO_2, which has an equilibrium fractional of $\delta^{13}C$ of −1.26 (at 11 °C) (Zhang et al., 1995).

The $\delta^{13}C$ values from the MW locations for both CH_4 and CO_2 were calculated by iteration and then the $\delta^{13}C$ confirmed by reference to the literature. The modern biogenic acetoclastic production of CH_4 has a median $\delta^{13}C$ value of −60 ‰, the thermogenic CH_4 has a median $\delta^{13}C$ value of −30 ‰ and the hydrogenotrophic production of CH_4 has a median $\delta^{13}C$ value of −80 ‰ (Negandhi et al., 2013). The modern terrestrial organic carbon source for CO_2 has a $\delta^{13}C$ value of −29 ‰. The coal carbon source for CO_2 has a $\delta^{13}C$ value of −23.5 ‰ (NEIF internal Scottish anthracite standard) with literature values between 23.7 ‰ and 27.4 ‰ (Suto and Kawashima, 2016). The limestone source has a $\delta^{13}C$ value of −6 ‰, with the main area of uncertainty around the $\delta^{13}C$ value for limestone, dependent on the source rock. Literature values ranged between −8.3 to +2.7 ‰ (Stanienda-pilecki, 2022), −12 to +4 ‰ (Keith and Weber, 1964) and −4 to +7 ‰ with European Namurian strata having values −3 to +6 ‰ (Bruckschen et al., 1999). The $\delta^{13}C$ for Scottish Carboniferous limestone, to the author's knowledge, has never been measured and the variation in literature values for limestone introduce uncertainty in the CO_2 $\delta^{13}C$ for this calculation.

2.5. Analysis

Pearson's correlation was applied to determine relationships between the GHG concentrations, water physiochemical properties and metal concentrations. Principal component analysis (PCA) was used to determine the level of correlation between the multiple variables within the survey, treating the different locations across the Midland Valley as different data points in a regional study. Values of $p < 0.05$ for correlation and difference tests were considered statistically significant.

3. Results

3.1. The Midland Valley's mine water physicochemical properties

MW outflows were characterized by high conductivity (400–4400 μS cm^{-1}), up to two orders of magnitude above that of the receiving river, slightly acidic to near-neutral conditions (pH 6–7), a low DO% content (6–25 %) and surface water temperatures between 9 °C and 16 °C.

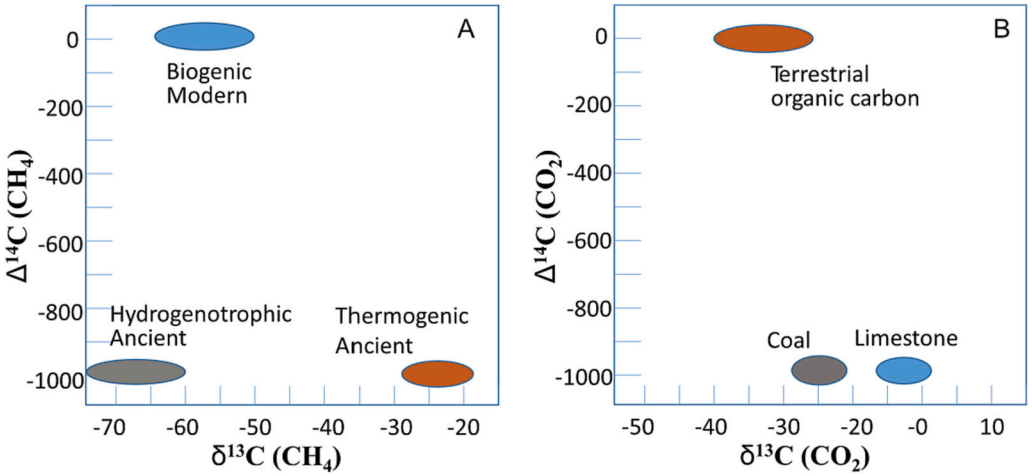

Fig. 3. Potential CO_2 and CH_4 sources in terms of their $\Delta^{14}C$ and $\delta^{13}C$ signature. Panel A represents signatures for three possible CH_4 sources; modern biogenic, ancient thermogenic and ancient hydrogenotrophic methanogenesis. Panel B represents signatures for three possible CO_2 sources: terrestrial organic carbon, ancient fossil carbon (limestone) and ancient CO_2 from coal. The actual samples will be a mixture of different sources. As both the CH_4 and CO_2 may have a modern or thermogenic/fossil carbon source and have been converted by differnt processes both $\Delta^{14}C$ and $\delta^{13}C$ measurements are required (Gonzalez Moguel et al., 2021; Keith and Weber, 1964; Iram et al., 2017; Lu et al., 2021).

Compared to receiving rivers MW outflows were high in DIC (40–200 mg l^{-1}), Mg^{2+} (10–170 mg l^{-1}), Ca^{2+} (50–290 mg l^{-1}), K^+ (2.5–25 mg l^{-1}) and SO_4^{2-} (25–610 mg l^{-1}). The total dissolved nitrogen was between 0.2 and 2.3 mg l^{-1} which most likely reflected the inflowing groundwater and organic carbon values ranged between 0 and 10 mg l^{-1} but most values were close to zero. The MW contained heavy metals with the concentrations ranging between; Fe (2–65 ppm), Mn (0.4–5.1 ppm), As (0.2–3.5 ppb), Co (0.1–225 ppb), Zn (1.8–125 ppb), Ni (0.5–300 ppb), Cu (0.5–35 ppb), Al (2.5–305 ppb) and B (36–1000 ppb). Other elements of concern such as Cd and Pb were low, in some cases below the limit of detection for the ICP-MS. Three sites were noted for particularly high concentrations of heavy metals. These were MA4 and MA6, which are outflows from the most recently flooded mines and had the highest concentrations of Fe and Mn and MA2 the only location

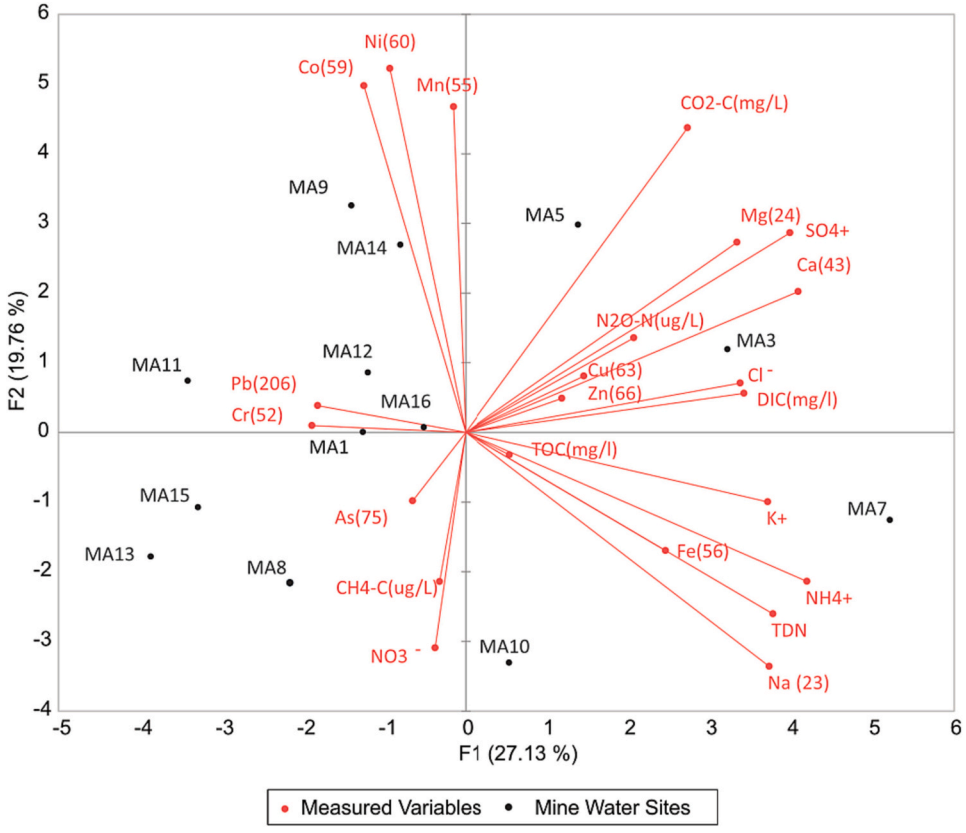

Fig. 4. Relationships between greenhouse gases and water chemical properties. MA1 to MA16 indicate the mine water locations sampled as part of this study (MA 2, 4 and 6 are not included as their high heavy metals concentrations dominate the analysis). Dissolved GHGs include: CO_2-C, CH_4-C and N_2O-N. Water chemical properties include: total dissolved nitrogen (TDN), dissolved organic carbon (DOC) and dissolved inorganic carbon (DIC), Cl^-, NO_3^-, SO_4^{2-}, Na^+, NH_4^+, K^+, Ca^{2+} and Mg^{2+} Co, Pb, Cr, Mn, As, Ni, Cu, Fe and Zn.

situated in the Productive Coal Measures (see Table 1), which had the highest concentrations of Co, Ni, Se, Hg and Zn. Location MA15 had the highest concentrations of Pb and As.

Due to the high number of variables PCA was undertaken to look at similarities between locations. However, the high metal content of sites, MA2, MA4 and MA6 dominated any analysis, indicating that time since abandonment and coal measure geology are important. To enable other relationships in this regional study to be determined, data from MA2, MA4 and MA6 were removed from the PCA in Fig. 4. Mg^{2+}, Ca^{2+}, DIC and CO_2 and SO_4^{2-} are highly correlated, consistent with high acidity from sulphuric acid dissolving the limestone in the coal measures. CH_4 is almost inversely correlated to Mg^{2+}, Ca^{2+}, DIC and CO_2 and SO_4^{2-} suggesting that conditions favourable to CO_2 production may inhibit methanogenesis. Fe is strongly correlated with total TDN and NH_4^+ and to a lesser extent Na^+ and K^+. Several metals were positively correlated to SO_4^{2-} and negatively correlated to pH across the range of MWs investigated including Mn, Fe, Co, Ni, Li, B, Zn, Rh, Sr and U. Conversely, Al, Ti, V, As, Cu, Se, Mo, Cs, Hg and Pb show no statistically significant correlations with either SO_4^{2-} or pH.

3.2. Sources of greenhouse gases in mine water

The GHG concentrations from the MW source locations were high, with $[CH_4]$ and $[CO_2]$ ranging from 20 to 215 $\mu g l^{-1}$ and 30 to 120 $mg\ l^{-1}$ respectively. Where MW sources were high in DO% and low in GHG, for example at MA2 and MA5, it is likely that some outgassing has already

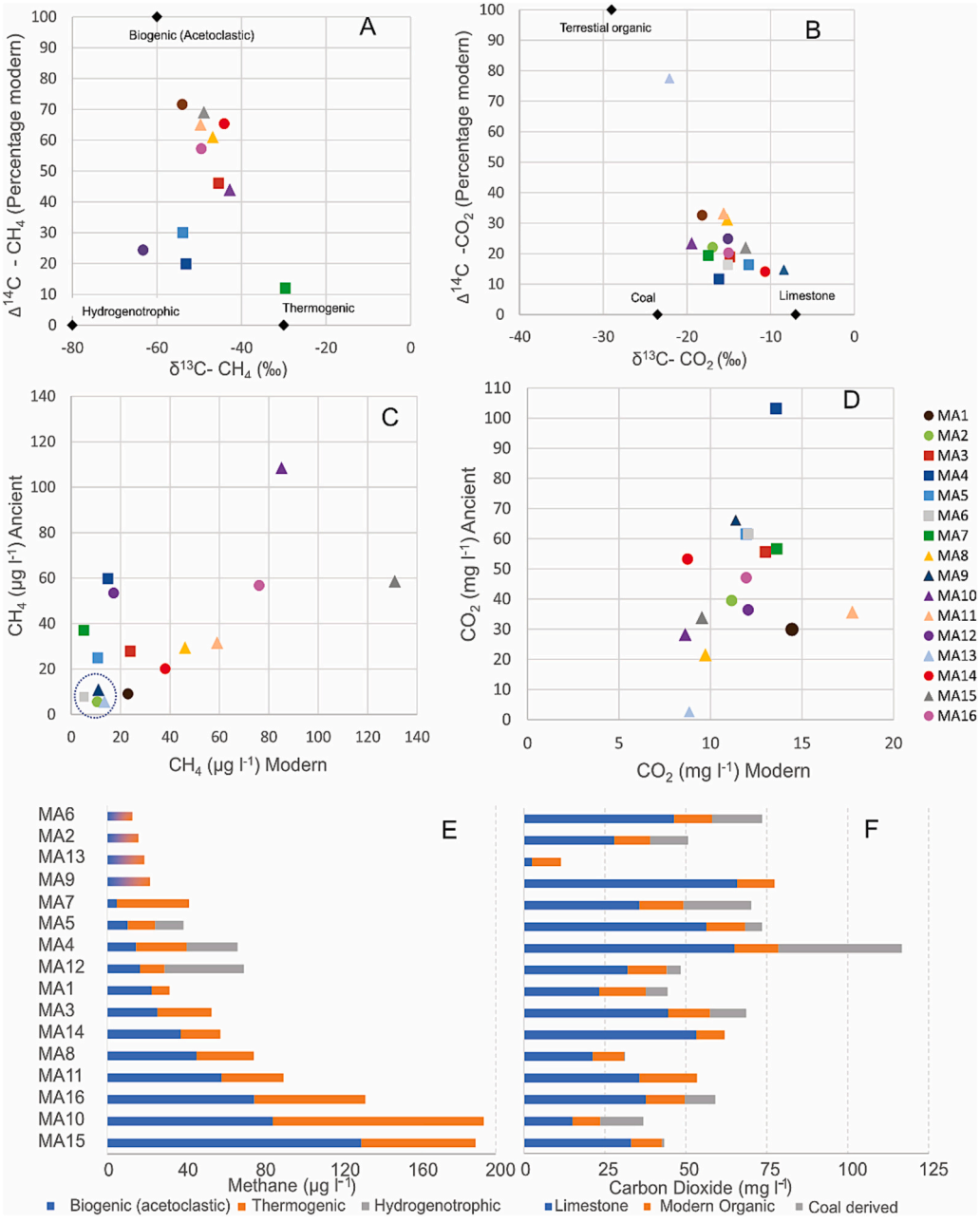

Fig. 5. Relationships between $\delta^{13}C$ and $\Delta^{14}C$ in mine water CH_4 and CO_2 for locations MA1 to MA16. Panel A shows the relationship between $\Delta^{14}C$ and $\delta^{13}C$ for CH_4 and Panel B for CO_2. Panel C shows relationship between the amount of modern and ancient CH_4 for MA1 to MA16 (Note sites MA 2, 6, 9, 13 (ringed), were not measured due to the low CH_4 concentration) and Panel D for CO_2. Triangles mark locations where sulphate concentrations in mine water are <100 mg l^{-1}, circles where sulphate concentrations are between 100 and 300 mg l^{-1} and squares where sulphate concentrations are between 300 and 600 mg l^{-1}. Panels E and F show the proportion of each source of CH_4 and CO_2 ranked by biogenic CH_4 concentrations (Note: panel E for MA2, 6, 9, and 13 the CH_4 source was not determined).

occurred during transport by underground pipe. The radiogenic and stable isotope data ($\Delta^{14}C$ and $\delta^{13}C$) were used to determine the sources of the CH_4 and CO_2, by using a three-source model (Fig. 3). Where isotopic characterisation was possible 51 % of the [CH_4] were of modern biogenic origin, 41 % from thermogenic origin and 8 % from hydrogenotrophic origin (Fig. 5 A, C and E). Conversely 65 % of the CO_2 is derived from limestone, 20 % from modern terrestrial organic carbon and 15 % from coal related carbon (Fig. 5 B, D and F). There is no correlation between the two 'modern carbon' concentrations for CH_4 and CO_2 (Table 2). Four locations (MA 8, 11, 14 and 15) appeared to contain no coal-based CH_4 and no coal-based CO_2 as indicated by their $\delta^{13}C$ values.

3.3. Greenhouse gas generation or consumption in reed pools

Measurements of $\Delta^{14}C$ and $\delta^{13}C$ were made on CH_4 and CO_2 from the reed pools and compared with that at the source (Fig. 1), using cascade (MA7 and MA10) and peroxide oxygenation (MA11 and MA12). The cascade at location MA7 was too efficient at outgassing GHGs to enable sufficient sample to be collected for this analysis.

There was no significant change in the $\Delta^{14}C$ of any reed pool samples compared to the source for CO_2, however the CO_2 $\delta^{13}C$ increased. For CH_4 there is a slight increase in percentage modern, particularly for MA12, which has extensive good quality reed pools and a similar increase in the CH_4 $\delta^{13}C$. This difference was particularly evident for the peroxide systems (MA11 and MA12) where energy is not being supplied by the cascade (Fig. 6).

3.4. Impact of oxygenation by cascade on greenhouse gas concentrations

At location MA7 water is pumped 0.25 km, from a well (source) site to a location where there is space and height for a 12 m gravity cascade to oxygenate the MW. GHGs were measured throughout the cascade, every 11 steps with the final location measured in the reed pool. The cascade increased DO from 17 % to 92 % and pH from 6.3 to 7.2. The [DIC] (assumed when measured to represent HCO_3^- only) decreased from 119 mg l^{-1} to 84 mg l^{-1}. [CH_4] decreased from 482 to 0.2 μg l^{-1} and the [CO_2] from 71 to 6.8 mg l^{-1}. Conversely the N_2O concentrations increased from 0.4 μg l^{-1} to 0.6 μg l^{-1} and then stabilised and further increased in the reed pools. This increase and stabilisation of [N_2O], indicated that N_2O was being produced rapidly within the water, probably stimulated by oxygen availability, with production and outgassing likely in equilibrium. The CH_4 concentration, unaffected by in-water processes could be used to estimate outgassing rate and would suggest that [N_2O-N] was on average 1.06 μg l^{-1} in the cascade (180 % higher than measured). The TDN concentrations in this sample were 1.6 mg l^{-1}, likely derived from groundwater. The outgassing of the CO_2 resulted in a pH change and changed the carbonate balance. Theoretical CO_2 values can be calculated from the pH and [DIC] and indicated that around 38 % of the CO_2 had outgassed before measurement.

3.5. The effectiveness of reed pools for removing heavy metals

Four treatment systems were selected to examine heavy metal removal, two with a cascade (MA7 and MA11) and two with peroxide

Table 2
Estimated concentrations of methane and carbon dioxide based on radiogenic and stable isotope ratios.

Location code(1)	Modern Biogenic CH_4 $\delta^{13}C$ −60 ‰,100 % modern		Ancient Thermogenic CH_4 $\delta^{13}C$ −30 ‰, 0 % modern		Hydrogenotrophic CH_4 $\delta^{13}C$ −80 ‰, 0 % modern		Modern Biogenic CO_2 $\delta^{13}C$ −29 ‰, 100 % modern		Ancient Limestone CO_2 $\delta^{13}C$ −6 ‰, 0 % modern		Ancient Coal CO_2 $\delta^{13}C$ −23.5 ‰, 0 % modern	
Sources	Proportion	(μgl^{-1})	Proportion	(μgl^{-1})	Proportion	(μgl^{-1})	Proportion	(mgl^{-1})	Proportion	(mgl^{-1})	Proportion	(mgl^{-1})
MA1S	0.72	22.9	0.23	7.5	0.05	1.6	0.33	14.6	0.52	23.2	0.15	6.7
MA2S							0.22	11.2	0.55	27.7	0.23	11.9
MA3S	0.46	23.8	0.51	26.3	0.03	1.6	0.19	13.0	0.65	44.5	0.16	11.1
MA4S	0.20	14.8	0.46	34.2	0.34	25.6	0.12	13.6	0.56	65.0	0.33	38.2
MA5S	0.30	10.7	0.40	14.4	0.30	10.6	0.16	12.0	0.77	56.3	0.07	5.2
MA6S							0.16	12.1	0.63	46.2	0.21	15.4
MA7S	0.12	5.0	0.88	37.1	0.00	0.0	0.19	13.6	0.51	35.7	0.30	21.0
MA8S	0.61	46.1	0.39	29.5	0.00	0.0	0.31	9.7	0.68	21.2	0.01	0.3
MA9S							0.15	11.4	0.85	66.1	0.00	0.0
MA10S	0.44	85.1	0.56	108.5	0.00	0.0	0.23	8.6	0.41	15.0	0.36	13.3
MA11S	0.65	59.0	0.35	31.4	0.00	0.3	0.33	17.8	0.67	35.7	0.00	0.0
MA12S	0.24	17.2	0.24	16.8	0.52	36.7	0.25	12.1	0.66	32.0	0.09	4.4
MA13S							0.78	8.8	0.22	2.6	0.00	0.0
MA14S	0.65	38.0	0.35	20.2	0.00	0.0	0.14	8.8	0.86	53.3	0.00	0.0
MA15S	0.69	130.9	0.31	58.7	0.00	0.0	0.22	9.5	0.76	33.1	0.02	0.7
MA16S	0.57	76.1	0.38	50.6	0.05	6.2	0.20	12.0	0.64	37.7	0.16	9.4
Average Source	0.47	40.4	0.42	36.3	0.09	6.9	0.25	11.8	0.62	37.2	0.13	8.6
Weighted source	0.51		0.41		0.08		0.20		0.65		0.15	

Reed Pools	Proportion	(μgl^{-1})	Proportion	(μgl^{-1})	Proportion	(μgl^{-1})	Proportion	(μgl^{-1})	Proportion	(μgl^{-1})	Proportion	(μgl^{-1})
MA10R	0.45	16.8	0.55	20.5	0.00	0.0	0.33	8.6	0.67	17.2	0.00	0.0
MA11R	0.66	18.6	0.34	9.6	0.00	0.0	0.26	8.2	0.75	24.0	0.00	0.0
MA12R	0.31	11.0	0.27	9.8	0.42	15.2	0.23	3.7	0.41	6.3	0.36	5.6

Notes
1. On the location code, S indicates this was a Source location, R indicates this was a reed pool location.
2. The following $\delta^{13}C$ values have been calculated for CH_4: modern biogenic acetoclastic production = −60 ‰, the thermogenic = −30 ‰ and the hydrogenotrophic production = −80 ‰.
3. The following $\delta^{13}C$ values have been calculated for CO_2: modern terrestrial organic carbon = − 29 ‰. The coal carbon source = − 23.5 ‰ and the Scottish Carboniferous limestone = −6
4. Both MA13 and MA9 may derive from opencast and appear to have a more positive $\delta^{13}C$ values for CO_2 from a fossil source (limestone) than at other sites.
5. The [CH_4] was too low at sites MA2 (16.2 μg l^{-1}) MA6 (13.1 μg l^{-1}) MA9 (22 μg l^{-1}) MA13 (19.2 μg l^{-1}) to measure the radiogenic and stable isotopes.
6. The 'average source' is the average proportion and concentration of each source, the 'weighted source' is proportion of each source accounting for the source concentrations.

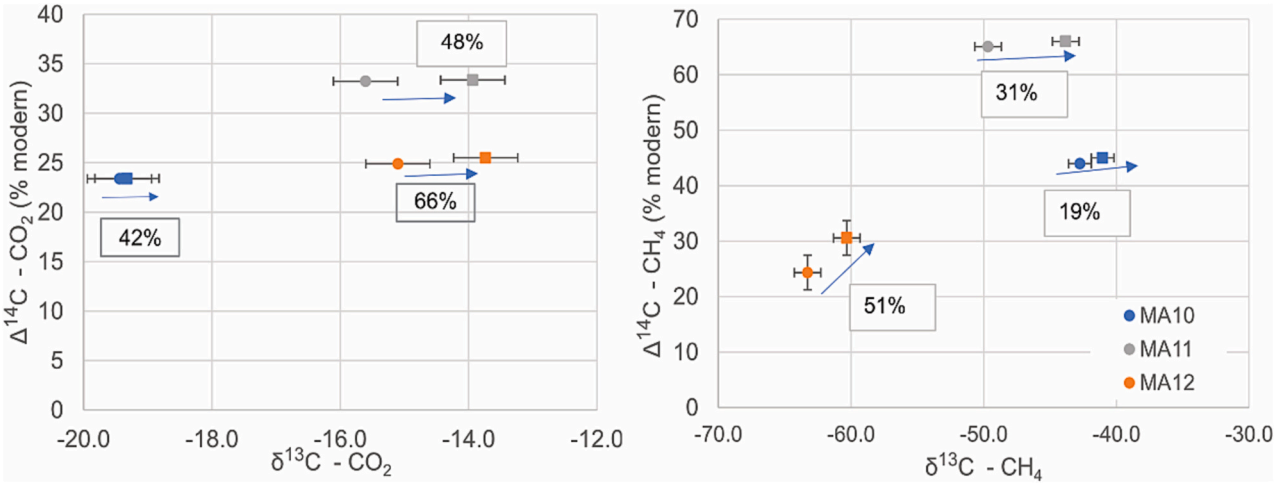

Fig. 6. Source to reed pool transition on $\Delta^{14}C$ and $\delta^{13}C$ composition. Location MA10 was oxygenated by a cascade system and locations MA11 and MA12 were oxygenated by peroxide. The circle indicates the location source and the square the location reed pool. The arrow showing the direction from source to reed pool. The percentage of the GHG remaining after transfer to the reed pool is indicated in the box for each system.

treatment (MA12 and MA13) (Fig. 1). Measurements were made at each stage of the treatment including; at source, after the cascade (if one was used), after the deep-water pool, in the main reed bed and at the outflow to the river (or after the second reed bed). Measurements included GHG concentrations and water physicochemical properties in addition to a range of metals. The cascade or peroxide systems increased the DO in the water causing Fe and As to precipitate (Fig. 7) demonstrated by the difference in the filtered and unfiltered concentrations. However, sufficient time was still required for fine particles of the insoluble Fe(III) and As(V) to settle to the bed. The Co, Ni and Mn are partly removed but do not appear to be precipitated by changes in their oxidations state as there is little difference between the filtered and unfiltered measurements. They may be partly removed by complexing or coagulation and then filtration by reeds or sedimentation. The reed pools had little impact on any other metals, for example Cu was not removed. The residence times within the systems varied, with that estimated for MA7, 11 and 12 in the order of days. At location MA11 there was a significant reduction in treatment residence time, which appeared insufficient for removal of metals, as the second reed bed was by-passed due to maintenance work and water was discharged to the river after the first reed bed (see Fig. 7).

4. Discussion

4.1. Causes of and variation in carbon dioxide and methane in mine water

This study is, to our knowledge, the first to investigate GHGs both in terms of source size and origin in the context of MW outflows. Across the locations in the Midland Valley for which stable and radiogenic isotopes were measured; 51 % of the CH_4 was of modern biogenic origin, 41 % from thermogenic origin and 8 % from hydrogenotrophic methanogenesis of coal origin. Conversely 65 % of the CO_2 was derived from limestone, 20 % from modern terrestrial organic carbon and 15 % from coal related carbon. There was no correlation between the CH_4 and CO_2 modern carbon concentrations, suggesting that factors other than availability of organic carbon are limiting these concentrations.

For biogenic CH_4 in MW, 70 % of the variation can be accounted for by considering the $[SO_4^{2-}]$ and the DO as per the equation in Fig. 8 A (R^2 = 0.78, *p*-value <0.001). Sulphate reducing bacteria (SRB) can outcompete methanogens, with rates of methanogenesis estimated at two orders of magnitude lower than rates of sulphate reduction, indicative of SRB having a higher substrate affinity for H_2 (Lovley and Klug, 1983; Kristjansson and Schönheit, 1983). The inverse relationship with DO may be an indication that anoxic conditions within the mine, increase CH_4 production. Alternatively, it more likely indicates that partial re-oxygenation of the MW has occurred prior to measurement. Our results from investigation of a cascade system at MA7 demonstrated that the rate of increase in DO% is proportional to the rate of decrease of GHGs by outgassing. If outgassing rather than mine environment is the main influence on measured DO, this indicates that MW $[CH_4]$ would be higher than measured, with a proportion of CH_4 already lost to the atmosphere. There is no statistically significant correlation between biogenic CH_4 concentration and DOC or time since abandonment, suggesting that time for organic material build up in the mine systems is not a major factor. Several of the deep mines sites have subsequently been mined by opencast including locations MA5, MA10 and MA15, and much of this opencast has undergone land restoration using sewage sludge. This is documented for the area above the MA15 outflow, the location with the highest measured biogenic $[CH_4]$, [Pb] and [As]. It is possible that this contamination is derived not from the mine but from the sewage sludge used in land restoration after 2017 (Eadha Enterprises, 2023; Scottish Power Energy Networks, 2019; Glasgow World, 2017). Sewage sludge could provide a source of modern carbon for biogenic methanogenesis or alternatively the bioavailable heavy metals contained in the sewage sludge could impact microbial metabolism. Metals can act as a catalysts for enzymes including methanogens. However, high metal concentrations can be toxic to microorganisms (Jarosławiecka and Piotrowska-Seget, 2022). As such adding sewage sludge in land restoration could have multiple, variable impacts on $[CH_4]$ in MW (Paulo et al., 2017).

Thermogenic CH_4 production occurs during coalification as increasing temperature and pressure drive CH_4 from the coal. The CH_4 production increases rapidly with increasing coal rank (based on hardness and volatility) although storage capacity is lower within high rank coals due to their lower porosity (Kholod et al., 2020b). The longwall mining approach, often used in the UK, leads to the collapse of overlying strata into the created void, reducing the stress in the overlying 150–200 m and underlying 40–70 m, with fracturing increasing the permeability of the coal. This together with the reduced pressure from mine ventilation has resulted in thermogenic CH_4 desorbing from the coal (Jones et al., 2004). Remaining coal seams within the strata, disturbed by mining continue to produce CH_4 at a low rate (Kershaw, 2005). It is hypothesised that once the mine is flooded, water pressure will restrict desorption of thermogenic CH_4, but water moving past the coal dissolved some thermogenic CH_4 probably dependent on the

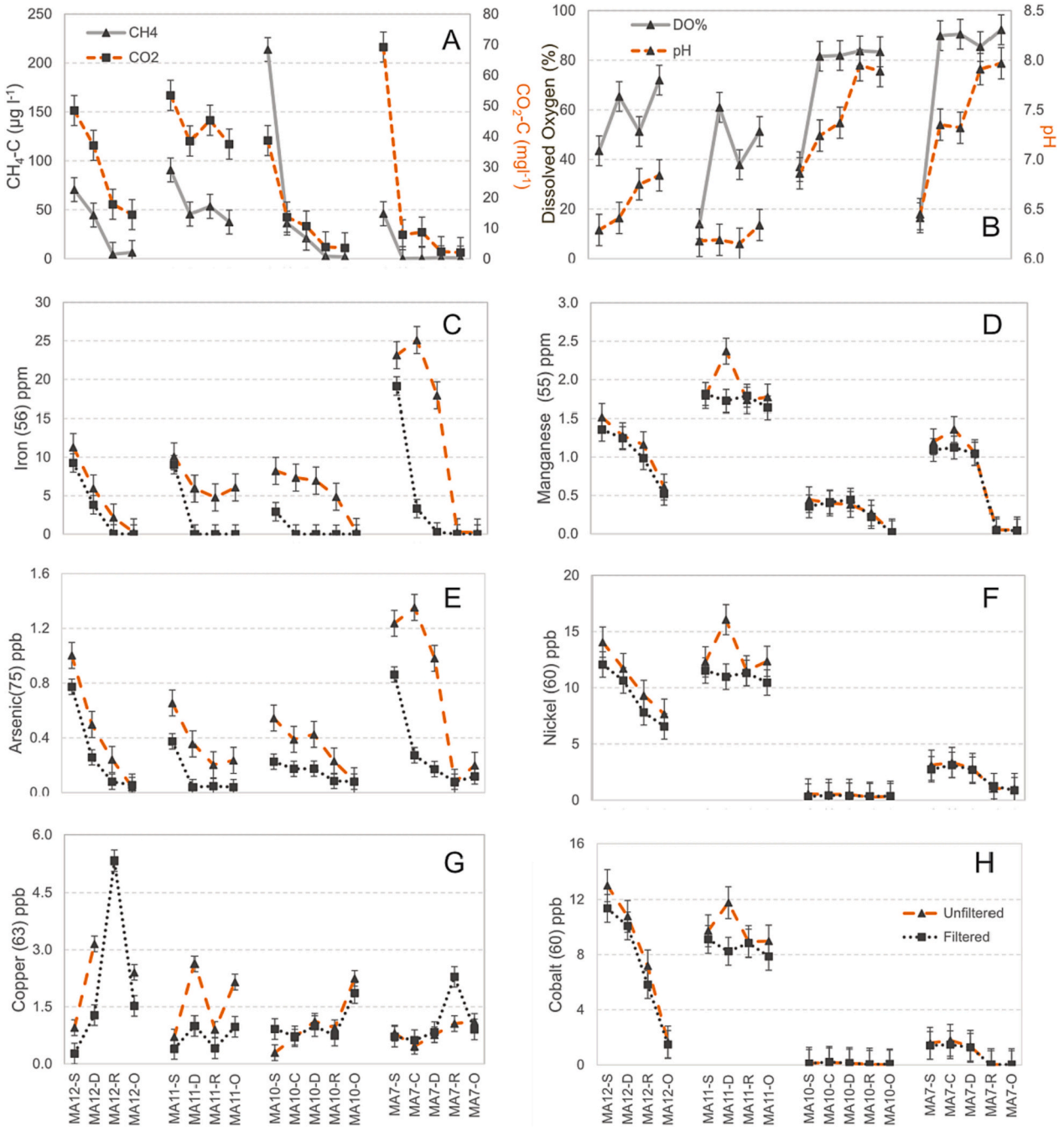

Fig. 7. Changes in heavy metal concentrations in treatment reed pools. Oxygenation is by a cascade for MA7 and MA10 and a peroxide drip for MA11 and MA12. The MA7 cascade is the most efficient oxygenation system. The measurement points through treatment systems included: S = source, C = end of cascade, D = exit from deep pool, R = reed pool, O = outflow. At the time of these measurements the second reef pool at MA11 was bypassed reducing the residence time.

remaining amount of coal and the CH_4 pressure, making up 41 % of the CH_4 in this region. Trapped thermogenic CH_4 could also be dissolved, with increasing water pressure. All MW contains thermogenic CH_4, with no statistically significant correlation with time since abandonment, suggesting an equilibrium is reached after flooding, with the amount of CH_4 dissolved, low compared to the size of the CH_4 reservoir. The best predictor of thermogenic CH_4 is pH and T_W as per the equation in Fig. 8 B ($R^2 = 0.66$, p-value <0.001).

Hydrogenotrophic methanogenesis is associated with the metabolism of short and long-chain alkanes and polyaromatic hydrocarbon (Gonzalez Moguel et al., 2021). This mechanism was only positively identified at locations MA 4, 5 and 12. Hydrogenotrophic CH_4 production requires CO_2 being produced from coal and reduced with H_2 as the electron donor (Park and Liang, 2016). However, the irregular structure of coal, the need for methoxylated aromatic compounds and complex microbial consortia under specific culture conditions and the more common occurrence in lower rank coals (Iram et al., 2017) are probably the reasons this biodegradation is limited. Hydrogenotrophy has been found to dominate in some low-temperature waters from coal seams with different coals having different methanogens present (Meslé et al., 2013). This mechanism does not appear very important in this region and there is insufficient data to determine causality, but it was found in both the most recent and the oldest abandoned mines.

CO_2 generated from the dissolution of limestone is the major mechanism for production of CO_2 in MW in the Midland Valley Scotland, as all coal measures are associated with limestone. The mechanism

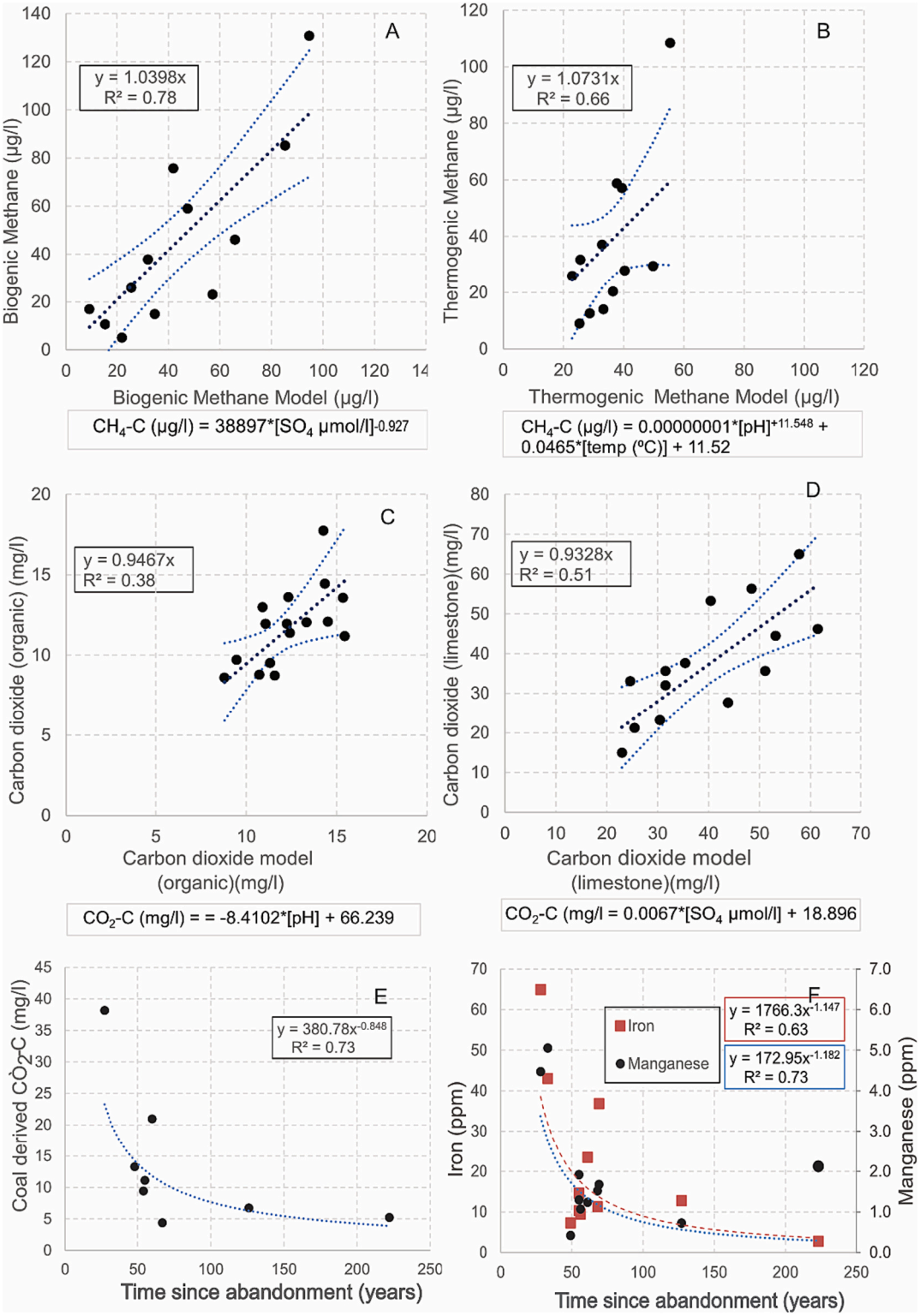

Fig. 8. Causal relationship for different CO_2 and CH_4 sources and metal concentration in mine water. Panel A - best fit relationship between biogenic CH_4 concentration and sulphate and dissolved oxygen. Panel B - best fit relationship between thermogenic CH_4 concentration and pH and temperature. Panel C - best fit relationship between biogenic CO_2 concentration and pH. Panel D - best fit relationship between CO_2 from limestone and sulphate concentration. Panel E - best fit relationship between CO_2 from coal and time since abandonment. Panel F - best fit relationship between iron and manganese concentration and time since abandonment. Confidence limits are for 95 %. Measurement standard error (σ) for modern CH_4 and CO_2 are in the order of 2 % and for the ancient CH_4 and CO_2 sources in the order of 5 %.

involves dissolution of FeS_2 forming sulphuric acid and this acidic environment accelerates the dissolution of limestone forming CO_2 (Eqs. (4) and (5)). The ratio of dissolved CO_2, carbonic acid (H_2CO_3) and bicarbonate (HCO_3^-) are dependent on the pH. As the pH increases the percentage of HCO_3^- also increases. In this context the strong negative correlation between limestone derived CO_2 and pH is predicted and is improved when the amount of DIC in solution is accounted for (R^2 = 0.51 and *p*-value <0.001). The concentration of CO_2 from limestone increased most strongly with [SO_4^{2-}] as per the equation in Fig. 8D (R^2 = 0.66 and p-value <0.001).

$$2FeS_2(s) + 2H_2O + 7O_2 \rightarrow 4H^+ + 4SO_4^{2-} + 2Fe^{2+} \quad (4)$$

$$CaCO_3 + H_2SO_4 \rightarrow CO_2 + H_2O + CaSO_4 \quad (5)$$

The relationship between biogenic CO_2 and pH is also significant as per the equation in Fig. 9C (R^2 = 0.38 and p-value <0.001), with the amount of biogenic CO_2 inversely correlated to pH. The pH is not known to impact DOC decomposition, although decomposition of organic matter leads to the production of acids, these acids are likely to be weak compared to the sulphuric acid produced from FeS_2. T_W was not found to be correlated with biogenic CO_2 although this is usually positively correlated with organic decomposition (Billett et al., 2007). While the proportion of biogenic CO_2 from terrestrial source changes the amount was relatively constant 8–18 mg l^{-1} and probably derived from the DOC in the water entering the mine, resulting in little remaining DOC.

The CO_2 derived from coal may also be the source of the hydrogenotrophic CH_4 found in some MW. Both the CO_2 and CH_4 data are consistent in suggesting that four locations (MA8, MA11, MA14 and MA15) have very little remaining coal and show no evidence for CO_2 from coal. The coal-based [CO_2] is inversely correlated with time since abandonment as in Fig. 8E (R^2 = 0.73 and p-value <0.001), suggesting that less CO_2 from this mechanism was produced with time, reducing to a low stable level (5 mg l^{-1}) after 100–200 years. This was the only identified GHG source to show a statistically significant relationship with time since abandonment. This would suggest that loss of dissolved CO_2 is significant compared to the CO_2 reservoir, leading to depletion of this source, probably due to the higher CO_2 solubility compared to that of CH_4. The reduction in coal-based CO_2 suggests hydrogenotrophic methanogenesis is less likely to become significant with time since abandonment.

4.2. Causes of heavy metals in mine waters

Heavy metals Fe and Mn had the highest concentrations, and both showed a significant reduction with time from flooding (Fe R^2 = 0.63, p-value <0.001) and (Mn R^2 = 0.73, p-value <0.001 (one value removed)) (Fig. 8F), with reduction to around half the initial concentration after 50-years. Although MA5 had an [Fe] of only 3 mg l^{-1} (about 5 % of the maximum value), the [Mn] was still 2.1 mg l^{-1} (about 42 % of the maximum value) after 230 years. MW outflow receiving rivers were often noted to have high [Mn] (SEPA, 2015). Li, B, K, Rb and Sb, available at much lower concentrations, showed similar significant reductions with time from flooding but this trend is not significant for any other metals in this region. Li, B, Mg, Ca, Mn, Fe, Rh, Sr and Ur showed a positive correlation with [SO_4^{2-}] and Co, Ni and Zn a negative correlation with pH, suggesting these are mainly dissolved by the low pH waters. However, there was no evidence that MW pH or [SO_4^{2-}] changed with time. Heavy metals are likely to continue to be dissolved if available in the mine. The reed pools were effective at removing Fe and As by oxidation to an insoluble form followed by precipitation. Mn, Co and Ni were also partly removed by the reed pool systems, most likely by adsorption (complexing or coagulation) to particles which subsequently settled, or by precipitation as carbonates and hydroxides which can occur at higher pHs (Nielsen et al., 2013). No other metals were removed. Treatment system effectiveness was associated with longer residence time and increasing pH and DO, with the high carbonate buffering likely reducing the overall dissolution of heavy metals.

4.3. Greenhouse gases from mine waters are all released to atmosphere

Where cascade systems are used the GHGs in the MW were release directly to atmosphere. The more effective the oxygenation cascade, the more GHGs were released. Where GHGs do enter the reed-pool systems there was little evidence of either CH_4 or CO_2 generation or consumption associated with the wetland environment. The change in the carbonate balance in a cascade resulted in some of the HCO_3^- being converted to CO_2 to replace that lost by rapid outgassing increasing carbon loss. In peroxide systems most of the CO_2 is lost to the atmosphere, but 30 % less HCO_3^- appears to be converted to CO_2, due to slower processing. For CH_4 there is a slight increase in the modern carbon within one treatment system (MA12). This could be indicative of biogenic methanogenesis within the read pools, but the reed pools are likely to be a weak source for methanogenesis while Fe^{2+} is present. Measurements of CH_4 $\delta^{13}C$ and CO_2 $\delta^{13}C$ from the reed pools and compared with that at the source showed an increase in all $\delta^{13}C$, which was particularly evident for the peroxide systems where energy is not being supplied by the cascade and was attributed to preferential loss of ^{12}C compared to ^{13}C during evasion processes.

In the low oxygen conditions in the mine, most of the nitrogen was in a reduced state, as ammonia, and in the presence of Fe^{2+}, a strong electron donor. As Fe^{2+} is oxidised to Fe^{3+} it donates electrons enabling nitrification (Wrage et al., 2001). Once oxygenation of the water occurred, N_2O was observed to increase, suggesting nitrification was main mechanism of nitrogen processing, as observed in the cascade at MA7. The N_2O concentration increased through the treatment process provided TDN was available. Reducing nitrogen in groundwater would reduce this GHG source.

Due to methodological limitations resulting in some outgassing prior to measurements, GHG measurements represent a minimum value. The average unweighted measured dissolved CO_2 concentrations across all sites was 58 mg l^{-1} and the average unweighted theoretical CO_2 concentrations was 91 mg l^{-1}, suggesting that on average 37 % of the supersaturated gases may be escaping prior to our measurements. The largest factor dictating the level of gas loss being the CO_2 saturation (R^2 = 0.51, *p*-value <0.001). At location MA4, which had the highest CO_2 concentration, bubbles were observed in the water as it reached the surface. A secondary factor appears to be distance of transfer, which was evident for locations MA2 an MA5 (Whitworth et al., 2012).

4.4. Estimates of the global warming potential in the mine waters

The estimated global warming potential (GWP) of the GHGs from MW are provided in Table 3 based on the assumptions: (1) all the GHGs from the MW outgas to atmosphere and are not consumed, (2) the distribution of GHGs across all sites is the same as the distribution measured, (3) the most likely number of potential sites in Scotland is 200 and (4) the average flow volume for all sites is not known, hence flow-weighted average concentrations were used with the average flow volume from the measurement sites (Table 3).

Our results show the legacy effects of mining related activities and their association with GHG production and climate change in the UK context, where most mining activity has ceased. The UK has over 900 abandoned coal mines (Fernando, 2011) but it is estimated there are over 48,000 in the USA (Manthos, 2016; OSMRE, 2016) and over 1 million mines globally (Candeias et al., 2019). Although climate change has prompted many countries to change their coal production strategies, worldwide coal consumption reached 7585 Mt. in 2017, with Asia continuing to expand its coal mining to drive economic development (International Energy Agency, 2018). Global coal consumption rebounded by 6 % to 7929 Mt. in 2021 resulting from the energy crisis (International Energy Agency, 2022). Given that mining remains a contemporary pressure, further investigation of GHG release and

Table 3
Global warming potential from mine water in Scotland.

	High	Mean	Low
Number of sources	200	150	100
Average flow (l/s)	90	70	50
Average CH4-C (μg l^{-1})	77	64	51
Average CO2-C (mg l^{-1})	80	64	46
Average N2O-N (μg l^{-1})	0.73	0.6	0.43
Total GWP (tones yr^{1}) (measured/calculated)	168,334/ 230,620	78,589/ 107,667	26,969/ 36,940
Percentage of Scotland GWP (%) (measured/calculated)	0.42/0.58 %	0.20/0.27 %	0.07/009 %

Notes
1. GWP for $CO_2 = 1$, $CH_4 = 28$ and $N_2O = 298$ (based on a 100-year time horizon) (Myhre et al., 2013).
2. The concentrations are estimated as the flow weighted average values from the survey.
3. High and low estimates are based on ±3 standard deviations from the mean for concentrations (mean).
4. 200 mine water sites have been identified (used as the upper estimate) however, the average flow volume for all sites is not known, hence the average flow from the measurement sites was used.
5. Scotland's emissions are 40.0 MtCO2e as reported for 2020 (Scottish Government, 2022).
6. The N_2O estimate is derived from N_2O measured at source but oxidations of the ammonia in MW would enable further N_2O production once the dissolved nitrogen is moved to the reed pools and rivers.
7. The calculated values include the estimated outgassing prior to measurement of 37 %.

management within such systems is important to inform closure procedures that minimise legacy emissions.

To enable translation of the MW GWP estimates from this regional study to a global GHG budget significant knowledge gaps need to be filled including: quantification of the total volume of MW from abandoned mines, their associated geology particularly with respect to the occurrence of carbonate and sulphur containing rocks and the impact of mining techniques and coal rank on the GHG sources identified. Additionally GHGs in MW from active mines has not be quantified but may be significant, for example China produces 4.5 billion $m^3\ yr^{-1}$ (Wang et al., 2021). Further research to characterise this potentially highly variable source would help with close the gap between bottom-up and top-down estimates of GHG emissions.

The 2006 IPCC Guidelines for National Greenhouse Gas inventories considers fugitive emissions from mining, including from abandoned mines (IPCC, 2006). It considers that abandoned mines are significant CH_4 emitters unless flooding inhibits release and allows emissions from completely flooded abandoned mines to be treated as negligible. Emissions related to GHGs dissolved in MW, are not considered including in the 2019 revision (IPCC, 2019). The focus for abandoned mines is on CH_4 emissions to air, while this study confirms that dissolved CO_2 can be the most significant GHG emission (97 % of the MW GWP) with dissolved CH_4 constituting the remainder. A section on future methodological development for fugitive emissions is presented in the Appendix (IPCC, 2019) which could be amended to include GHG dissolved in MW with the focus on mines where limestone and high sulphur rocks are present in the geology. Where carbonate-based rocks are used to treat acid MW, associated CO_2 should also be included as a fugitive emission.

For Scotland the 2020 deep mine abandoned mine methane (AMM) projections were 0.05 $MtCO_2e$ with no AMM utilisation (Fernando, 2011). The annual estimates of GHG emissions from this study for MW in Scotland range from 0.03 to 0.35 $MtCO_2e$. The mean estimate of GHG production from AMW in Scotland derived from this study is 0.1 $MtCO_2e$, twice that from the AMM, suggesting this term should be accounted for in the fugitive emission calculation towards inventory reporting.

5. Conclusions

The origins of the dissolved CH_4 and CO_2 in MW from the abandoned coal mines were effectively determined by the application of $\Delta^{14}C$ and $\delta^{13}C$ measurements, with three different sources distinguished for both CH_4 and CO_2. The concentrations of the different CH_4 and CO_2 sources varied considerably dependant on the MW location, with [SO_4^{2-}] the biggest factor influencing both [CH_4] and [CO_2]. Sulphate inhibited methanogenesis but increased CO_2 from the dissolution of limestone. The flooding of the mine enabled dissolution of limestone and conversion of DOC to produce CO_2, whereas CH_4 production was significantly reduced by flooding. The main source of CH_4 was biogenic production from modern carbon in the water, but thermogenic CH_4 was still significant with neither CH_4 nor CO_2 impacted by time since abandonment.

The different treatment processes, specifically the use of peroxide or cascade, and varied use of pools and reed beds had only a small impact on the final GHG emissions to atmosphere. The cascade systems released GHGs more rapidly reducing any opportunity for later removal, and resulting in increased CO_2 emissions (30 %) due to the conversion of HCO_3^- to CO_2 to restore the carbonate equilibrium. Reed pools could act as a source of biogenic CH_4 although the effect was small likely due to inhibition by metal ions. Configuration of the reed pools had a significant impact on heavy metal removal with residence times in the order of days required to allow settling of precipitated ions. The treatment by oxygenation and reed pools was most effective for the removal of Fe and As, which relies on oxidation and precipitation of higher valence state compounds and to a lesser extent Co, Ni and Mn, but no other metals were removed. The MWs [Fe] and [Mn] decreased by half, typically 50-years after mine inundation although some MWs exhibited persistent residual metal contamination.

In Scotland many MW sites are treated, but this is not be the case globally with contamination from tailings and acid mine drainage a significant cause of global pollution (Carvalho, 2017) and causing significant damage to biodiversity (Ayangbenro et al., 2018). As coal mines are abandoned it is advantageous to utilise AMM, with the most suitable mines having minimal water ingress and the ability to reduce water and air ingress with the largest quantities of AMM recovered in the first 10 years after abandonment (UNECE, 2019). However, most mines will eventually flood creating MW, although the prevention of air ingress could reduce pyrites oxidation. While mines are often engineered to facilitate AMM production, mines also need to be engineered to prevent significant MW pollution, which would be most effectively done before or as the mine is abandoned. Modifications to inhibit sulphuric acid generation processes would be required and would reduce CO_2 generation and the dissolution of heavy metals but could increase biogenic CH_4. While the latter would be a relatively small GHG impact when compared to any CO_2 reduction it could also support AMM. Dissolved MW CH_4 could perhaps be recovered from the MW, in similar ways to that applied to wastewater (GMI, 2023). Two approaches to reduce sulphuric acid generation include, use of engineered SBRs (Muyzer and Stams, 2008; Ayangbenro et al., 2018), although the isolation of acid tolerant SBRs, may be required (Magowo et al., 2020) to avoid the use of neutralising agency such a calcium carbonate and, coating the pyrites within the mine while in operation as each area is mined and before pyrites oxidation and mine flooding. Coating of mine walls would be viable to reduce acid generation hence preventing the dissolution of both metals and carbonate rock from future abandoned mines (Liu et al., 2017) and could be tested for its compatibility with AMM recovery.

This novel work has contributed information about the sources and controls of GHG fluxes in MW and identified the need to quantify and include this emissions term in GHG budgets.

Supplementary data to this article can be found online at https://doi.org/10.1016/j.scitotenv.2023.167371.

Funding

This work was financially supported by the Natural Environment Research Council (NERC) studentship through the IAPETUS 2 Doctoral Training Partnership Grant No. NE/S007431/1.

The radiogenic and stable carbon isotope analysis was financially supported by a National Environmental Isotope Facility (Part of the Natural Environmental Research Council), Grant Number 2513.0422 and samples were measured by the NEIF Radiocarbon Laboratory in East Kilbride.

CRediT authorship contribution statement

Alison M. Brown Conceptualization, Funding acquisition, Methodology, Investigation (Field work, Laboratory Work) Data curation, Formal analysis, Writing-Original draft preparation, Visualization, Project administration

Dr. Adrian M. Bass Conceptualization, Funding acquisition, Supervision, Reviewing and Editing

Dr. Mark H. Garnett Conceptualization, Funding acquisition, Investigation (Laboratory work - isotope measurement), Reviewing and Editing

Prof. Ute Skiba Supervision, Reviewing and Editing

Dr. John M. Macdonald Supervision, Reviewing and Editing

Dr. Amy E. Pickard Conceptualization, Funding acquisition, Investigation (Field work) Supervision, Reviewing and Editing

Declaration of competing interest

The authors declare that they have no known competing financial interests or personal relationships that could have appeared to influence the work reported in this paper.

Data availability

The data is published at EIDC and referenced in the paper - https://doi.org/10.5285/49daf07b-cfbe-48d1-8889-1adafe410a2e

Acknowledgements

The authors would like to thank The Coal Authority and Severn Trent Services for allowing access to and supporting sampling at their MW treatment sites for the purpose of making these measurements.

The authors would like to thank Edinburgh University for undertaking the ICP-MS analysis.

All photographs in the supplementary data were taken by Alison M. Brown.

References

Acharya, B.S., Kharel, G., 2020. Acid mine drainage from coal mining in the United States – an overview. J. Hydrol. 588 (April), 125061. https://doi.org/10.1016/j.jhydrol.2020.125061.

Alhamed, M., Wohnlich, S., 2014. Environmental impact of the abandoned coal mines on the surface water and the groundwater quality in the south of Bochum, Germany. Environ. Earth Sci. 72 (9), 3251–3267. https://doi.org/10.1007/s12665-014-3230-9.

Ayangbenro, A.S., Olanrewaju, O.S., Babalola, O.O., 2018. Sulfate-reducing bacteria as an effective tool for sustainable acid mine bioremediation. Front. Microbiol. 9 (AUG), 1–10. https://doi.org/10.3389/fmicb.2018.01986.

Billett, M.F., Moore, T.R., 2008. Supersaturation and evasion of CO_2 and CH_4 in surface waters at Mer Bleue peatland, Canada. Hyrdol. Process. 22 (November 2008), 2044–2054. https://doi.org/10.1002/hyp.

Billett, M.F., Garnett, M.H., Harvey, F., 2007. UK peatland streams release old carbon dioxide to the atmosphere and young dissolved organic carbon to rivers. Geophys. Res. Lett. 34 (23), 2–7. https://doi.org/10.1029/2007GL031797.

British Geological Survey, 2023. Geoindex Onshore, Geoindex Onshore - MapApps2 [online] Available from: https://mapapps2.bgs.ac.uk/geoindex/home.html.

Brown, A., Garnett, M., Eades, L., Pickard, A.E., 2023. Greenhouse gas, carbon isotopes, water physio-chemical properties and metal concentrations from mine water outflows in the Midland Valley, Scotland, 2022. In: NERC EDS Environ. Inf. Data Cent. https://doi.org/10.5285/49daf07b-cfbe-48d1-8889-1adafe410a2e.

Brown, M., 2019. U.S. mining sites dump 50 million gallons of fouled wastewater daily, Public Broadcast. Serv [online] Available from: https://www.pbs.org/newshour/nation/u-s-mining-sites-dump-50-million-gallons-of-fouled-wastewater-daily.

Bruckschen, P., Oesmann, S., Veizer, J., 1999. Isotope stratigraphy of the European carboniferous: proxy signals for ocean chemistry, climate and tectonics. Chem. Geol. 161 (1), 127–163. https://doi.org/10.1016/S0009-2541(99)00084-4.

Candeias, C., Ávila, P., Coelho, P., Teixeira, J.P., 2019. Mining activities: health impacts. Encycl. Environ. Health 415–435. https://doi.org/10.1016/B978-0-12-409548-9.11056-5.

Carvalho, F.P., 2017. Mining industry and sustainable development: time for change. Food Energy Secur. 6 (2), 61–77. https://doi.org/10.1002/fes3.109.

De Voogt, P., 2020. Reviews of Contamination and Toxicology.

Dean, M.T., Browne, M.A.E., Waters, C.N., Powell, J.H., 2011. A lithostratigraphical framework for the Carboniferous successions of northern Great Britain (onshore). Br. Geol. Surv. Res. Rep. 174. RR/09/01.

Dhir, B., 2018. Biotechnological Tools for Remediation of Acid Mine Drainage (Removal of Metals From Wastewater and Leachate). Elsevier Inc.

Eadha Enterprises, 2023. Glentaggart Opencast Mine Woodland Project [online] Available from: http://www.eadha.co.uk/projects/331_glentaggart_opencast_mine_woodland_project.

Energy Institute, 2023. Statistical Review of World Energy.

Fernando, S., 2011. Update of Estimated Methane Emissions From UK Abandoned Coal Mines, (May) [online] Available from: www.wspenvironmental.com.

Findlay, S., McDowell, W.H., Fischer, D., Pace, M.L., Caraco, N., Kaushal, S.S., Weathers, K.C., 2010. Total carbon analysis may overestimate organic carbon content of fresh waters in the presence of high dissolved inorganic carbon. Limnol. Oceanogr. Methods 8 (MAY), 196–201. https://doi.org/10.4319/lom.2010.8.196.

Fleming, C., Morrison, K., Robba, L., Reynolds, J., Wright, I.A., 2021. 14-Month water quality investigation of coal mine discharge on Two Rivers in NSW, Australia: implications for environmental regulation. Water Air Soil Pollut. 232 (3) https://doi.org/10.1007/s11270-021-05020-7.

Fleming, C., Belmer, N., Reynolds, J.K., Robba, L., Davies, P.J., Wright, I.A., 2022. Legacy contamination of river sediments from four decades of coal mine effluent inhibits ecological recovery of a polluted world heritage area river. Water Air Soil Pollut. 233 (1) https://doi.org/10.1007/s11270-021-05487-4.

Florence, K., Sapsford, D.J., Johnson, D.B., Kay, C.M., Wolkersdorfer, C., 2016. Iron-mineral accretion from acid mine drainage and its application in passive treatment. Environ. Technol. (United Kingdom) 37 (11), 1428–1440. https://doi.org/10.1080/09593330.2015.1118558.

Furukawa, Y., Inubushi, K., Furukawa, Y., 2004. Effect of application of iron materials on methane and nitrous oxide emissions from two types of paddy soils. Soil Sci. Plant Nutr. 50 (6), 917–924. https://doi.org/10.1080/00380768.2004.10408554.

Garnett, M.H., Billett, M.F., Gulliver, P., Dean, J.F., 2016. A new field approach for the collection of samples for aquatic 14CO2 analysis using headspace equilibration and molecular sieve traps: the super headspace method. Ecohydrology 9 (8), 1630–1638. https://doi.org/10.1002/eco.1754.

Gauci, V., Gowing, D.J.G., Hornibrook, E.R.C., Davis, J.M., Dise, N.B., 2010. Woody stem methane emission in mature wetland alder trees. Atmos. Environ. 44 (17), 2157–2160. https://doi.org/10.1016/j.atmosenv.2010.02.034.

Glasgow World, 2017. Human sewage sludge plan for Dalquhandy opencast site, Glas. World [online] Available from: https://www.glasgowworld.com/news/human-sewage-sludge-plan-for-dalquhandy-opencast-site-2083872.

GMI, 2023. Global Methane Initiative (GMI) - Municipal Wastewater Technical Group, 2023 [online] Available from: https://www.globalmethane.org/biogas/ww.aspx.

Gonzalez Moguel, R., Vogel, F., Ars, S., Schaefer, H., Turnbull, J., Douglas, P., 2021. Using carbon-14 and carbon-13 measurements for source attribution of atmospheric methane in the Athabasca Oil Sands Region. Atmos. Chem. Phys. Discuss. 1–21. https://doi.org/10.5194/acp-2021-622 (August).

Hamilton, S., 2006. Prediction of Dissolved Gas Concentrations in Water at Atmospheric Equilibrium, pp. 3–6 [online] Available from: https://lter.kbs.msu.edu/docs/linx/linx2/linx2_dissolved_gas_headspace_equilibration_calcs.pdf.

Hedin, R.S., Hedin, B.C., 2016. The complicated role of CO_2 in mine water treatment. In: Proc. IMWA 2016, Freiberg/Germany, 3, pp. 844–849 (TU).

IEA, 2020. Methane Tracker 2020 [online] Available from: www.iea.org/reports/methane-tracker-2020.

International Energy Agency, 2018. Market Report Series: Coal 2018 [online] Available from: www.iea.org/t&c/.

International Energy Agency, 2022. Coal 2022 [online] Available from: https://iea.blob.core.windows.net/assets/91982b4e-26dc-41d5-88b1-4c47ea436882/Coal2022.pdf.

IPCC, 2006. IPCC Guidelines for National Greenhouse Gas Inventories - Volume 2 Energy - Chapter 4 Fugitive Emissions.

IPCC, 2019. In: Calvo Buendia, E., Tanabe, K., Kranjc, A., Baasansuren, J., Fukuda, M., Ngarize, S., Osako, A., Pyrozhenko, Y., Shermanau, P., Federici, S. (Eds.), 2019 Refinement to the 2006 IPCC Guidelines for National Greenhouse Gas Inventories - Volume 2 Energy - Chapter 4 Fugitive Emissions, IPCC Natl. Greenh. Gas Invent. Program, 2, pp. 56–74. https://doi.org/10.1007/978-1-4939-6911-1.

Iram, A., Akhtar, K., Ghauri, M.A., 2017. Coal methanogenesis: a review of the need of complex microbial consortia and culture conditions for the effective bioconversion of coal into methane. Ann. Microbiol. 67 (3), 275–286. https://doi.org/10.1007/s13213-017-1255-5.

Jarosławiecka, A.K., Piotrowska-Seget, Z., 2022. The effect of heavy metals on microbial communities in industrial soil in the area of Piekary Śląskie and Bukowno (Poland). Microbiol. Res. (Pavia) 13 (3), 626–642. https://doi.org/10.3390/microbiolres13030045.

Jarvis, A.P., 2006. The role of dissolved carbon dioxide in governing deep coal mine water quality and determining treatment process selection. In: 7th Int. Conf. Acid Rock Drain. 2006, ICARD - Also Serves as 23rd Annu. Meet. Am. Soc. Min. Reclam, 1, pp. 833–843. https://doi.org/10.21000/jasmr06020833.
Johnston, D., Potter, H., Jones, C., Rolley, S., Watson, I., Pritchard, J., 2008. Abandoned Mines and the Water Environment.
Jones, N.S., Holloway, S., Creedy, D.P., Garner, K., Smith, N.J.P., Browne, M.A.E., Durucan, S., 2004. UK Coal Resource for New Exploitation Technologies Final Report UK Coal Resource for New Exploitation Technologies Final Report.
Keith, M.L., Weber, J.N., 1964. Carbon and oxygen isotopic composition of selected limestones and fossils. Geochim. Cosmochim. Acta 28 (10−11), 1787–1816. https://doi.org/10.1016/0016-7037(64)90022-5.
Kershaw, S., 2005. Development of a Methodology for Estimating Methane Emissions From Abandoned Coal Mines in the UK, IMC White, p. 109 [online] Available from: file://tsn.tno.nl/Data/SV/sv-066092/Refworks/Kershaw(2005).pdf.
Kholod, N., Evans, M., Pilcher, R.C., Roshchanka, V., Ruiz, F., Coté, M., Collings, R., 2020a. Global methane emissions from coal mining to continue growing even with declining coal production. J. Clean. Prod. 256 (February), 120489. https://doi.org/10.1016/j.jclepro.2020.120489.
Kholod, N., Evans, M., Pilcher, R.C., Roshchanka, V., Ruiz, F., Coté, M., Collings, R., 2020b. Global methane emissions from coal mining to continue growing even with declining coal production. J. Clean. Prod. 256 https://doi.org/10.1016/j.jclepro.2020.120489.
Koschorreck, M., Prairie, Y.T., Kim, J., Marcé, R., 2021. Technical note: CO_2 is not like CH4- limits of and corrections to the headspace method to analyse pCO_2 in fresh water. Biogeosciences 18 (5), 1619–1627. https://doi.org/10.5194/bg-18-1619-2021.
Kristjansson, J.K., Schönheit, P., 1983. Why do sulfate-reducing bacteria outcompete methanogenic bacteria for substrates? Oecologia 60 (2), 264–266. https://doi.org/10.1007/BF00379530.
Laanbroek, H.J., 2010. Methane emission from natural wetlands: interplay between emergent macrophytes and soil microbial processes. A mini-review. Ann. Bot. 105, 141–153. https://doi.org/10.1093/aob/mcp201.
Leslie, A.G., Browne, M.A.E., Cain, T., Ellen, R., 2016. From threat to future asset—the legacy of opencast surface-mined coal in Scotland. Int. J. Coal Geol. 164, 123–133. https://doi.org/10.1016/j.coal.2016.06.017.
Li, P., 2018. Mine water problems and solutions in China. Mine Water Environ. 37 (2), 217–221. https://doi.org/10.1007/s10230-018-0543-z.
Liu, Y., Hu, X., Xu, Y., 2017. PropS-SH/SiO_2 nanocomposite coatings for pyrite oxidation inhibition to control acid mine drainage at the source. J. Hazard. Mater. 338, 313–322. https://doi.org/10.1016/j.jhazmat.2017.05.043.
Lopez, M., Sherwood, O.A., Dlugokencky, E.J., Kessler, R., Giroux, L., Worthy, D.E.J., 2017. Isotopic signatures of anthropogenic CH4 sources in Alberta, Canada. Atmos. Environ. 164, 280–288. https://doi.org/10.1016/j.atmosenv.2017.06.021.
Lovley, D.R., Klug, M.J., 1983. Sulfate reducers can outcompete methanogens at freshwater sulfate concentrations. Appl. Environ. Microbiol. 45 (1), 187–192.
Lu, X., Harris, S.J., Fisher, R.E., France, J.L., Nisbet, E.G., Lowry, D., Röckmann, T., Van Der Veen, C., Menoud, M., Schwietzke, S., Kelly, B.F.J., 2021. Isotopic signatures of major methane sources in the coal seam gas fields and adjacent agricultural districts, Queensland, Australia. Atmos. Chem. Phys. 21 (13), 10527–10555. https://doi.org/10.5194/acp-21-10527-2021.
Lyu, X., Yang, K., Fang, J., 2022. Utilization of resources in abandoned coal mines for carbon neutrality. Sci. Total Environ. 822, 153646. https://doi.org/10.1016/j.scitotenv.2022.153646.
Macdonald, J.A., Fowler, D., Hargreaves, K.J., Skiba, U., Leith, I.D., Murray, M.B., 1998. Methane emission rates from a northern wetland; response to temperature, water table and transport. Atmos. Environ. 32 (19), 3219–3227.
Magowo, W.E., Sheridan, C., Rumbold, K., 2020. Global co-occurrence of acid mine drainage and organic rich industrial and domestic effluent: biological sulfate reduction as a co-treatment-option. J. Water Process Eng. 38 (September), 101650. https://doi.org/10.1016/j.jwpe.2020.101650.
Manthos, D., 2016. Mapping Abandoned Coal Mines, Sky Truth [online] Available from: https://skytruth.org/2015/10/mapping-abandoned-coal-mines/.
Mayumi, D., Mochimaru, H., Tamaki, H., Yamamoto, K., Yoshioka, H., Suzuki, Y., Kamagata, Y., Sakata, S., 2016. Methane production from coal by a single methanogen. Sci. Res. Rep. 354 (6309), 222–225.
Meslé, M., Dromart, G., Oger, P., 2013. Microbial methanogenesis in subsurface oil and coal. Res. Microbiol. 164 (9), 959–972. https://doi.org/10.1016/j.resmic.2013.07.004.
Millero, F.J., Graham, T.B., Huang, F., Bustos-Serrano, H., Pierrot, D., 2006. Dissociation constants of carbonic acid in seawater as a function of salinity and temperature. Mar. Chem. 100 (1–2), 80–94. https://doi.org/10.1016/j.marchem.2005.12.001.
Muyzer, G., Stams, A.J.M., 2008. The ecology and biotechnology of sulphate-reducing bacteria. Nat. Rev. Microbiol. 6 (6), 441–454. https://doi.org/10.1038/nrmicro1892.
Myhre, G., Shindell, D., Bréon, F., Collins, W., Fuglestvedt, J., Huang, J., Koch, D., Lamarque, J., Lee, D., Mendoza, B., Nakajima, T., Robock, A., Stephens, G., Takemura, T., Zhang, H., 2013. Anthropogenic and natural radiative forcing. In: Climate Change 2013: The Physical Science Basis. Contribution of Working Group I to the Fifth Assessment Report of the Intergovernmental Panel on Climate Change. Cambridge University Press, Cambridge, United Kingdom and New York, NY, USA.
Negandhi, K., Laurion, I., Whiticar, M.J., Galand, P.E., Xu, X., Lovejoy, C., 2013. Small thaw ponds: an unaccounted source of methane in the Canadian high Arctic. PLoS One 8 (11). https://doi.org/10.1371/journal.pone.0078204.
Nielsen, E., Greve, K., Ladefoged, O., 2013. Cobalt(II), Inorganic and Soluble Salts - Evaluation of Health Hazards and Proposal of a Health Based Quality Criterion for Drinking Water.
OSMRE, 2016. Abandoned mine land inventory system, U.S. Dep. Inter [online] Available from: https://amlis.osmre.gov/Summaries.aspx.
Park, S.Y., Liang, Y., 2016. Biogenic methane production from coal: a review on recent research and development on microbially enhanced coalbed methane (MECBM). Fuel 166, 258–267. https://doi.org/10.1016/j.fuel.2015.10.121.
Paulo, L.M., Ramiro-Garcia, J., van Mourik, S., Stams, A.J.M., Sousa, D.Z., 2017. Effect of nickel and cobalt on methanogenic enrichment cultures and role of biogenic sulfide in metal toxicity attenuation. Front. Microbiol. 8 (JUL), 1–12. https://doi.org/10.3389/fmicb.2017.01341.
Peng, S., Lin, X., Thompson, R.L., Xi, Y., Liu, G., Hauglustaine, D., Lan, X., Poulter, B., Ramonet, M., Saunois, M., Yin, Y., Zhang, Z., Zheng, B., Ciais, P., 2022. Wetland emission and atmospheric sink changes explain methane growth in 2020. Nature 612 (7940), 477–482. https://doi.org/10.1038/s41586-022-05447-w.
Saria, L., Shimaoka, T., Miyawaki, K., 2006. Leaching of heavy metals in acid mine drainage. Waste Manag. Res. 24 (2), 134–140. https://doi.org/10.1177/0734242X06063052.
Schwarzenbach, R.P., Egli, T., Hofstetter, T.B., Von Gunten, U., Wehrli, B., 2010. Global water pollution and human health. Annu. Rev. Environ. Resour. 35, 109–136. https://doi.org/10.1146/annurev-environ-100809-125342.
Scottish Government, 2022. Scottish Greenhouse Gas Statistics 2020. An Off. Stat. Publ. Scotl. [online] Available from: https://www.gov.scot/news/scottish-greenhouse-gas-statistics-2020/
Scottish Power Eneregy Networks, 2019. Kennoxhead to Coalburn Overhead Line Minerals Report.
SEPA, 2015. Water Classification Hub, Crown Copyright. SEPA Licens. Number 100016991 [online] Available from: https://www.sepa.org.uk/data-visualisation/water-classification-hub/.
Sheoran, A.S., Sheoran, V., 2006. Heavy metal removal mechanism of acid mine drainage in wetlands: a critical review. Miner. Eng. 19 (2), 105–116. https://doi.org/10.1016/j.mineng.2005.08.006.
Stanienda-pilecki, K., 2022. Stable isotopes carbon C13 and oxygen O18 as indicators of Triassic limestone sedimentation environment and diagenesis. Res. Sq. 1–21.
Stearns, M., Tindall, J.A., Cronin, G., Friedel, M.J., Bergquist, E., 2005. Effects of coal-bed methane discharge waters on the vegetation and soil ecosystem in Powder River Basin, Wyoming. Water Air Soil Pollut. 168 (1–4), 33–57. https://doi.org/10.1007/s11270-005-0588-z.
Suto, N., Kawashima, H., 2016. Global mapping of carbon isotope ratios in coal. J. Geochem. Explor. 167, 12–19. https://doi.org/10.1016/j.gexplo.2016.05.001.
The Coal Authority, 2017. Coal mine water treatment [online] Available from: https://www.gov.uk/government/collections/coal-mine-water-treatment (Accessed 20 May 2020).
Thisani, S.K., Von Kallon, D.V., Byrne, P., 2020. Geochemical classification of global mine water drainage. Sustainability 12 (24), 1–16. https://doi.org/10.3390/su122410244.
Tomiyama, S., Igarashi, T., 2022. ScienceDirect the potential threat of mine drainage to groundwater resources. Environ. Sci. Health 27, 100347. https://doi.org/10.1016/j.coesh.2022.100347.
Topp, E., Pattey, E., 1997. Soils as sources and sinks for atmospheric methane. Can. J. Soil Sci. 77 (2), 167–178. https://doi.org/10.4141/s96-107.
UNECE, 2019. Best Practice Guidance for Effective Methane Recovery and Use From Abandoned Coal Mines.
Verburg, R., Bezuidenhout, N., Chatwin, T., Ferguson, K., 2009. The Global Acid Rock Drainage Guide (GARD Guide). Mine Water Env. 28, 305–310. https://doi.org/10.1007/s10230-009-0078-4.
Vesper, D.J., Moore, J.E., Adams, J.P., 2016. Inorganic carbon dynamics and CO2 flux associated with coal-mine drainage sites in Blythedale PA and Lambert WV, USA. Environ. Earth Sci. 75 (4), 1–14. https://doi.org/10.1007/s12665-015-5191-z.
Wang, X., Gao, Y., Jiang, X., Zhang, Q., Liu, W., 2021. Analysis on the characteristics of water pollution caused by underground mining and research progress of treatment technology. Adv. Civ. Eng. https://doi.org/10.1155/2021/9984147.
Watten, B.J., Sibrell, P.L., Schwartz, M.F., 2005. Acid neutralization within limestone sand reactors receiving coal mine drainage. Environ. Pollut. 137 (2), 295–304. https://doi.org/10.1016/j.envpol.2005.01.026.
Whitworth, K., England, A., Parry, D., 2012. Overview of Mine Water in the UK Coalfields Project: Advice on Mine Water recovery and Mine Gas [online] Available from: www.wyg.com.
Winterdahl, M., Wallin, M.B., Karlsen, R.H., Laudon, H., Öquist, M., Lyon, S.W., 2016. Decoupling of carbon dioxide and dissolved organic carbon in boreal headwater streams. J. Geophys. Res. Biogeosci. 121 (10), 2630–2651. https://doi.org/10.1002/2016JG003420.
Wrage, N., Velthof, G.L., Van Beusichem, M.L., Oenema, O., 2001. Role of nitrifier denitrification in the production of nitrous oxide. Soil Biol. Biochem. 33 (12−13), 1723–1732. https://doi.org/10.1016/S0038-0717(01)00096-7.
Wright, I.A., Belmer, N., Davies, P.J., 2017. Coal mine water pollution and ecological impairment of one of Australia's most 'protected' high conservation-value rivers. Water Air Soil Pollut. 228 (3) https://doi.org/10.1007/s11270-017-3278-8.

Younger, P.L., 1997. The longevity of minewater pollution: a basis for decision-making. Sci. Total Environ. 194/195, 457–466. https://doi.org/10.1016/S0048-9697(96)05383-1.

Younger, P.L., 2001. Mine water pollution in Scotland: nature, extent and preventative strategies. Sci. Total Environ. 265 (1–3), 309–326. https://doi.org/10.1016/S0048-9697(00)00673-2.

Zhang, J., Quay, P.D., Wilbur, D.O., 1995. Carbon isotope fractionation during gas-water exchange and dissolution of CO_2. Geochim. Cosmochim. Acta 59 (1), 107–114. https://doi.org/10.1016/0016-7037(95)91550-D.